

General Disclaimer

One or more of the Following Statements may affect this Document

- This document has been reproduced from the best copy furnished by the organizational source. It is being released in the interest of making available as much information as possible.
- This document may contain data, which exceeds the sheet parameters. It was furnished in this condition by the organizational source and is the best copy available.
- This document may contain tone-on-tone or color graphs, charts and/or pictures, which have been reproduced in black and white.
- This document is paginated as submitted by the original source.
- Portions of this document are not fully legible due to the historical nature of some of the material. However, it is the best reproduction available from the original submission.



Battelle

Columbus Laboratories

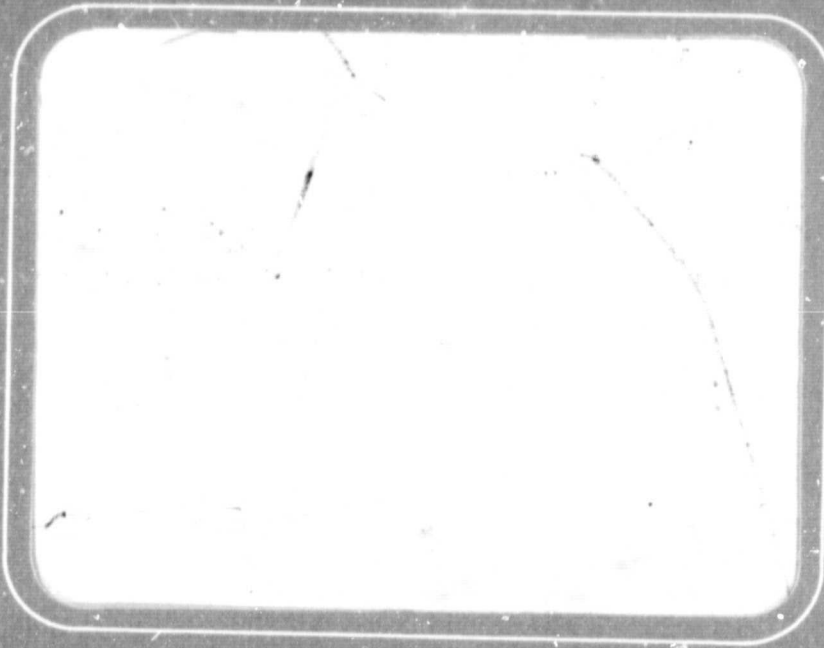
(NASA-CR-170857) ULTRAPURE GLASS OPTICAL
WAVEGUIDE: DEVELOPMENT IN MICROGRAVITY BY
THE SOL GEL PROCESS Annual Progress Report
(Battelle Columbus Labs., Ohio.) 69 p
HC A04/MF A01

N83-34052

Unclass
41995

CSSL 11B G3/27

Report



ANNUAL PROGRESS REPORT
(Contract No. N/S8-3489~~A~~) 34894

on

ULTRAPURE GLASS OPTICAL WAVEGUIDE:
DEVELOPMENT IN MICROGRAVITY BY THE SOL GEL PROCESS

to

NATIONAL AERONAUTICS AND SPACE ADMINISTRATION
GEORGE C. MARSHALL SPACE FLIGHT CENTER
HUNTSVILLE, ALABAMA

AUGUST 12, 1983

by

Shyama P. Mukherjee, J. C. Debsikdar, and T. Beam

BATTELLE
Columbus Laboratories
505 King Avenue
Columbus, Ohio 43201

TABLE OF CONTENTS

	<u>Page</u>
SUMMARY	1
INTRODUCTION	3
EXPERIMENTAL WORK AND RESULTS	5
Selection of Oxide Systems and Compositions	5
Preparation of Gels and Gel Monoliths	6
SiO ₂ -GeO ₂ System	6
GeO ₂ -PbO System	10
SiO ₂ -TiO ₂ System	10
Drying of Gels and Gel Monoliths	10
Characterization of Gels	13
SiO ₂ -GeO ₂ System	13
GeO ₂ -PbO System	19
Conversion of Gels to Glasses	50
SiO ₂ -GeO ₂ System	50
GeO ₂ -PbO System	50
Preparation of Gel-Derived Glasses	51
Preparation of Glasses by Melting	
Conventional Batch Material	53
Characterization of Glasses in the	
GeO ₂ -PbO System	53
Thermal Treatment of Levitated Gel Monolith	59
CONCLUSIONS	62

LIST OF TABLES

	<u>Page</u>
Table 1. Gel Compositions in the SiO ₂ -GeO ₂ System	7
Table 2. Gel Compositions in the GeO ₂ -PbO System	7
Table 3. Gel Preparation Parameters (SiO ₂ -GeO ₂ System)	8
Table 4. Gel Preparation Parameters (GeO ₂ -PbO System)	11
Table 5. Gel Preparation Parameters (SiO ₂ -TiO ₂ System)	12
Table 6. Results of X-Ray Powder Diffraction Patterns	20
Table 7. Infrared Absorption Frequencies of Lead Germanate Gels	27
Table 8. Infrared Absorption Frequencies of Lead Acetate, Lead Oxide, and Germanium Oxide (Frequency Range 4000 to 400 cm ⁻¹)	32
Table 9. Description of Gels Studied for Their Crystallization Behavior	34
Table 10. DTA Peaks of Lead Germanate Gels	39
Table 11. d Spacings of PG 1(a) and PG 1(c) Gels After Different Thermal Treatments	44
Table 12. d Spacings of PG 2(b) and PG 3(b) Gels	46
Table 13. d Spacings of Compounds in the GeO ₂ -PbO System	47
Table 14. Melting and Annealing Temperatures of Lead Germanate Glasses	54
Table 15. Chemical Compositions of PG 1 Glasses	54
Table 16. DTA of Gel-Derived and Conventional Lead Germanate Glass	57

LIST OF FIGURES

Figure 1. Schematic Diagram Showing the Arrangements for Supercritical Drying of Gel Monolith.	14
---	----

LIST OF FIGURES (Continued)

	<u>Page</u>
Figure 2. Differential Thermal Analysis of SG 1 Gel	15
Figure 3. Differential Thermal Analysis of SG 2 Gel	16
Figure 4. Differential Thermal Analysis of SG 5 Gel	17
Figure 5. Differential Thermal Analysis of SG 6 Gel	18
Figure 6. Scanning Electron Photomicrograph of PG 1(b) Gel Dried at 70 C	21
Figure 7. Infrared Spectrum of PG 1(a) Gel Dried at 70 C	22
Figure 8. Infrared Spectrum of PG 1(b) Gel Dried at 70 C	23
Figure 9. Infrared Spectrum of PG 1(c) Gel Dried at 70 C	24
Figure 10. Infrared Spectrum of PG 2(b) Gel Dried at 70 C	25
Figure 11. Infrared Spectrum of PG 3(b) Gel Dried at 70 C	25
Figure 12. Infrared Spectrum of Supercritically Dried PG 1(c) Gel	26
Figure 13. Infrared Spectrum of Lead Acetate Trihydrate	28
Figure 14. Infrared Spectrum of Lead Oxide (PbO)	29
Figure 15. Infrared Spectrum of Noncrystalline Germanium Oxide	30
Figure 16. Infrared Spectrum of Crystalline Germanium Oxide	31
Figure 17. Differential Thermal Analysis of PG 1(a) Gel	35
Figure 18. Differential Thermal Analysis of PG 1(b) Gel	36
Figure 19. Differential Thermal Analysis of Supercritically Dried PG 1(c) Gel	37
Figure 20. Differential Thermal Analysis of PG 1(c) Gel	37
Figure 21. Differential Thermal Analysis of PG 2(b) Gel	38
Figure 22. Differential Thermal Analysis of PG 3(b) Gel	38

LIST OF FIGURES (Continued)

	<u>Page</u>
Figure 23. Differential Thermal Analysis of Lead Acetate (Basic)	41
Figure 24. Differential Thermal Analysis of Noncrystalline Germanium Oxide	41
Figure 25. Heating Schedule for the Sintering of Gel Monolith of Composition SG 2	51
Figure 26. Thermal Dilatometric Curve of a Gel Monolith of Composition SG 2	52
Figure 27. Infrared Spectrum of Gel-Derived PG 1 Glass, 1200 C/3 HR	56
Figure 28. Infrared Spectrum of Conventionally Melted PG 1 Glass, 1200 C/5 HR	56
Figure 29. Differential Thermal Analysis of Conventional PG 1 Glass	58
Figure 30. Differential Thermal Analysis of Gel-Derived PG 1 Glass	58
Figure 31. Hot Zone vs Specimen Temperatures During Levitated Sintering	61

Annual Progress Report

ON

ULTRAPURE GLASS OPTICAL WAVEGUIDE: DEVELOPMENT IN MICROGRAVITY BY THE SOL GEL PROCESS

to

National Aeronautics and Space Administration
George C. Marshall Space Flight Center

from

Battelle's Columbus Laboratories

August 12, 1983

SUMMARY

During the current reporting period, investigations were conducted mainly to develop the sol gel process for the preparation of homogeneous gels in three binary oxide systems and to study the glass forming ability of certain compositions in the selected oxide systems ($\text{SiO}-\text{GeO}_2$, GeO_2-PbO , and $\text{SiO}_2-\text{TiO}_2$), based on their potential importance in the design of optical waveguide at longer wavelengths. The compositions chosen for the selected oxide systems were:

$\text{SiO}_2-\text{GeO}_2$ System (Compositions in Weight Percent). 95 SiO_2 · 5 GeO_2 ; 90 SiO_2 · 10 GeO_2 ; 44 SiO_2 · 56 GeO_2 ; and 20 SiO_2 · 80 GeO_2 .

GeO_2-PbO System (Composition in Mol Percent). 90 GeO_2 · 10 PbO ; 67 GeO_2 · 33 PbO ; and 50 GeO_2 · 50 PbO .

SiO₂-TiO₂ System (Composition in Weight Percent). 94 SiO₂ · 6 TiO₂.

The results of the present work are summarized below.

- Noncrystalline gels and gel monoliths could be prepared in all the oxide systems.
- Gel monoliths in the SiO₂-GeO₂ system were supercritically dried without any loss of integrity. However, the integrity of gel monoliths in the GeO₂-PbO system were lost during supercritical drying due to structural breakdown. The supercritical drying experiment was not performed on the gel monoliths of the SiO₂-TiO₂ composition.
- Except Composition 95 SiO₂ · 5 GeO₂ all other composition gels in the SiO₂-GeO₂ system showed crystallization tendency on thermal treatment at higher temperatures (800-1200 C). However, all composition gels in the GeO₂-PbO system showed crystallization tendency at much lower temperatures. The nature of crystalline phases were found to depend on the composition, the gel preparation behavior, and the drying technique. The SiO₂-TiO₂ composition gel was not studied for its crystallization behavior.
- Glasses could be prepared from lead germanate gels by melting.
- Lead germanate glass composition could be effectively controlled by the sol gel route.
- The crystallization behaviors of gel-derived and conventional lead germanate glasses were different.
- Levitation experiments with porous gel monoliths were investigated. Porous gel monoliths in the SiO₂-GeO₂ system were levitated in an aquatic levitator located at Intersonics, Inc.

INTRODUCTION

The containerless melting of glass in the reduced gravity environment of space will open up a unique approach to producing glasses uncontaminated by containers during melting. This approach will offer the following advantages:

- Preparation of ultrapure optical glasses in multicomponent systems by eliminating contamination from transition metal impurities in the container during melting.
- Formation of new glasses that crystallize due to heterogeneous nucleations originating in the container walls during melting.
- Improved homogeneity in the glass system where, in the absence of gravity-induced segregation, the densities of the constituent oxides are significantly different.

However, because of the absence of gravity-induced convection currents, the homogenization of multicomponent glass using conventional raw materials or glass batches will be difficult in the microgravity environment. Multicomponent, homogeneous, noncrystalline metal oxide gels can be promising starting material for melting glasses in the space environment.

Considering the advantages of the containerless melting of gels for preparing glasses, the objectives of the present program were to:

1. Develop procedures to prepare gels important or potentially important in optical waveguide applications.
2. Study gel homogeneity and gel-derived glasses in selected oxide systems.
3. Study the glass forming ability of certain compositions in the selected oxide systems by containerless melting of homogeneous, multicomponent, noncrystallized gels.
4. Study the influence of container impurities on the glass forming ability of certain compositions in the selected oxide systems by containerless melting of homogeneous, multicomponent gels and gel monoliths.
5. Study the influence of container impurities on the glass forming ability of selected compositions in the selected oxide systems.

6. Perform containerless melting of multicomponent gels and gel monoliths for investigating nucleation and crystallization kinetics.

The oxide systems selected for investigation in the first stage of the program were:

1. SiO₂-GeO₂
2. GeO₂-PbO/Bi₂O₃
3. SiO₂-TiO₂.

Current interest in optical fiber design is centered on the 1 to 1.8 micron region where both the attenuation and dispersion of silica-based waveguides are at a minimum. At longer wavelengths, even lower intrinsic attenuations are possible, primarily due to a lower scatter contribution, Rayleigh scattering decreasing as λ^{-4} . Hence, the oxide systems mentioned above are important for their potential applications to optical communication technology. But the preparation of homogeneous and ultrapure optical glasses in these systems is difficult by the conventional techniques. Because of high melting temperatures and inhomogeneity of compositions, it is difficult to prepare high quality optical glasses in the SiO₂-GeO₂ and SiO₂-TiO₂ systems. Hence, the containerless melting of noncrystalline, homogeneous gels and gel monoliths in these systems could lead to the preparation of ultrapure optical glasses. The crystallization tendency and high reactivity of glasses in the GeO₂-PbO/Bi₂O₃ systems are obstacles for studying the glass forming ability of the compositions in this system. The containerless melting of homogeneous gels in these systems will eliminate the heterogeneous nucleation sites introduced during melting in a container, making it possible to study the intrinsic glass forming ability of gels. Moreover, the incorporation of certain cations (such as Ti⁺⁴, Ge⁺⁴) in fourfold coordination into the glass structure can be achieved more effectively by the sol gel process, making it possible to expand the glass forming zone of the oxide systems containing these cations.

EXPERIMENTAL WORK AND RESULTS

The experimental work at this stage of the program was divided into the following activities:

- Selection of oxide systems and compositions
- Preparation of gels and gel monoliths
- Drying of gels and gel monoliths
- Characterization of gels
- Conversion of gels to glass
 - by melting of gel powders
 - by sintering of gel monoliths
- Melting of conventional glass batches
- Light scattering studies of glasses
- Levitation of porous gel monoliths and thermal treatment during levitation.

Selection of Oxide Systems and Compositions

The following oxide systems were chosen:

1. $\text{SiO}_2\text{-GeO}_2$
2. $\text{GeO}_2\text{-PbO/Bi}_2\text{O}_3$
3. $\text{SiO}_2\text{-TiO}_2$.

The first system was selected because of its importance in glass optical communication technology. The prime objective was to prepare homogeneous gels and glasses having higher concentrations of GeO_2 in order to investigate the influence of GeO_2 on the homogeneity and crystallization tendency of gels in this system.

The molten glasses in the $\text{GeO}_2\text{-PbO/Bi}_2\text{O}_3$ systems have high chemical reactivity. Since it is difficult to prepare glasses uncontaminated by containers, it is also difficult to improve the intrinsic glass forming ability of the compositions in this system. The containerless melting of homogeneous gels in this system will eliminate the heterogeneous nucleation sites introduced during melting in a container, thereby making it possible to study the intrinsic glass forming ability of the compositions.

In the third system, the objective was to prepare highly homogeneous gels having Ti^{+4} ions in fourfold coordination state.

SiO₂-GeO₂ System. To investigate the effect of GeO₂ concentration on the chemical and structural homogeneity of gels in the SiO₂-GeO₂ system, several compositions with increasing GeO₂ concentrations were chosen (Table 1).

GeO₂-PbO/Bi₂O₃ System. The compositions in the GeO₂-PbO system selected to study gel preparation procedures are given in Table 2. No work has yet been done in the GeO₂-Bi₂O₃ system.

SiO₂-TiO₂ System. The composition chosen for the preliminary investigation in the SiO₂-TiO₂ system was SiO₂ 94 • TiO₂ 6 (weight percent).

Preparation of Gels and Gel Monoliths

SiO₂-GeO₂ System. Gels and gel monoliths were prepared by several procedures by varying the process parameters. The objective was to determine the influence of starting compounds, pH, the ratio of water to alkoxides, and solution concentration on the homogeneity and processing behavior of gels. Basically, two different approaches to gel preparation were developed. The first approach incorporated partial hydrolysis using 1 mole H₂O per alkoxide and acid (HCl) as the catalyst. The second approach contained a complete hydrolysis using 5 moles H₂O per alkoxide using a base (NH₄OH) as catalyst. Both approaches yielded transparent gels and gel monoliths, except in cases of high solution concentration or high GeO₂ percentage. Specific details of the process parameters are given in Table 3.

The starting chemicals for the gel preparations were:

<u>Source</u>	<u>Oxide</u>
Tetraethoxysilane	SiO ₂
Tetramethoxysilane	SiO ₂
Germanium ethoxide	GeO ₂

TABLE 1. GEL COMPOSITIONS IN THE SiO₂-GeO₂ SYSTEM

Composition Number	Composition	
	SiO ₂ (Weight Percent)	GeO ₂ (Weight Percent)
SG1	95	5
SG2	90	10
SG3	85	15
SG4	80	20
SG5	44	56
SG6	20	80

TABLE 2. GEL COMPOSITIONS IN THE GeO₂-PbO SYSTEM

Composition Number	Composition (Mol Percent)	
	GeO ₂	PbO
PG1	90	10
PG2	67	33
PG3	50	50

TABLE 3. GEL PREPARATION PARAMETERS (SiO₂-GeO₂ SYSTEM)

Composition Number	Composition	P. #	Starting Material	H ₂ O Add'n mole H ₂ O / mole Si(OR) ₄	Final pH	Gelation Time	Sol'n Conc. (in percent)	Drying Condition	Sol'n Add'n
SG1	SiO ₂ -5GeO ₂	18	Si(OC ₂ H ₅) ₄	1, 4	2-3	45 min	10	air	HF
SG1	SiO ₂ -5GeO ₂	18	Si(OC ₂ H ₅) ₄	1, 4	2-3	45 min	10	autoclave	HF
SG1	SiO ₂ -5GeO ₂	45	Si(OC ₂ H ₅) ₄	1, 4	2-3	2-3 days	10	autoclave	--
SG2	SiO ₂ -10GeO ₂	45	Si(OC ₂ H ₅) ₄	2, 8	2-3	2-4 days	5	air	--
SG2	SiO ₂ -10GeO ₂	45	Si(OC ₂ H ₅) ₄	1, 4	2-3	2-3 days	10	autoclave	--
SG2	SiO ₂ -10GeO ₂	51	Si(OCH ₃) ₄	1, 4	2-3	4 days	10	autoclave	--
SG2	SiO ₂ -10GeO ₂	54	Si(OCH ₃) ₄	5	6-7	<2 hr	4	air	NH ₄ OH
SG2	SiO ₂ -10GeO ₂	54	Si(OCH ₃) ₄	5	6-7	<2 hr	4	autoclave	NH ₄ OH
SG3	SiO ₂ -15GeO ₂	23	Si(OC ₂ H ₅) ₄	1, 4	≤2	2-4 days	10	air	--
SG4	SiO ₂ -20GeO ₂	22	Si(OC ₂ H ₅) ₄	1, 4	≤2	2-4 days	10	air	--
SG5	SiO ₂ -20GeO ₂	50	Si(OCH ₃) ₄	1, 4	2-3	<20 hr	10	air	--
SG5	SiO ₂ -20GeO ₂	73	Si(OCH ₃) ₄	1, 4	2-3	<24 hr	10	15 min hydrolysis	--
SG5	SiO ₂ -20GeO ₂	73	Si(OCH ₃) ₄	1, 4	2-3	<24 hr	10	3 hr hydrolysis	--
SG6	SiO ₂ -56GeO ₂	77	Si(OCH ₃) ₄	1, 4	<2	2 min	10	air	--
SG6	SiO ₂ -80GeO ₂	78	Si(OCH ₃) ₄	1, 4	<2	2 min	10	air	--

ORIGINAL PAGE IS OF POOR QUALITY

Approach I. Equal volumes of alkoxysilane and alcohol were poured into a beaker, heated to ~ 40 C and stirred continuously. Acidified water (0.003 mol HCl/mol alkoxysilane and 1 mol H_2O /mol alkoxysilane) was added to partially hydrolyze the silane. Stirring continued at ~ 40 C for some time until the pH was less than 2. After cooling the solution to room temperature, 10:1 volume mixture of ethanol and germanium ethoxide was added to the solution and stirring continued for $\sim 1/2$ hour at room temperature. The pH was again less than 2. Hydrolysis of all alkoxides was completed by adding 4 moles of water per mole of alkoxides in ethanol to the above solution. The solution continued to be stirred until gelation occurred, or the solution was cast into a teflon mold for monolithicity studies. The final pH of the transparent rigid gel was between 2 and 3.

Approach II. A 3:1 volume ratio of methanol to methoxysilane was combined in a beaker and stirred for ~ 10 minutes at room temperature. Dilute ammonium hydroxide (0.0001 mol NH_4OH /mol methoxysilane and 1 mol H_2O /mol methoxysilane) was added to partially hydrolyze the methoxysilane. The solution was stirred for ~ 45 minutes when the pH was ~ 8 . A 10:1 volume mixture of ethanol to germanium ethoxide was added to the solution. The pH was ~ 5 . Immediately, hydrolysis was completed by adding aqueous ammonium hydroxide diluted in ethanol (4 moles H_2O /mol of alkoxide and 0.0001 mole NH_4OH /mole of alkoxide). The final pH of the transparent or translucent gel (in instances of high solution concentration) was ~ 7 .

Drying of Gels. The polymeric solution was poured into a mold to obtain monolithic shape. Generally the molds are made of tetrafluoroethylene (TFE) teflon. As the solution gels and is aged in the mold, the monolith shrinks. The teflon mold provides frictionless surface that does not induce stresses or cracking in the gel monolith during aging.

Gels were dried in two different ways. In the first, gels were dried in covered polyethylene pans at room temperature for approximately one month in an alcohol-water atmosphere. The gels shrank radially ~ 50 -60 vol. percent. In the second, the gels were supercritically dried in an autoclave at 243 C and ~ 1100 psi for complete evacuation of alcohol from the monolithic gels. The gels were aged for approximately one week at room temperature

before autoclaving to allow for initial shrinkage away from the mold wall. There was no observed volume shrinkage.

GeO₂-PbO System. Gels and gel monoliths were prepared in several ways by varying the process parameters. The objective was to investigate the influence of process parameters on the crystallization behavior of gels. The compositions prepared by different procedures are shown in Table 4. The differences in the preparation procedure relate to the differences in the molar ratio of water to germanium ethoxide and/or concentration of oxides in the solution.

SiO₂-TiO₂ System. A number of polymeric solutions of composition SiO₂ 94 · TiO₂ 6 (weight percent) were prepared by varying the process parameters, namely, catalyst concentration, water concentration, and temperature and duration of the initial hydrolysis of alkoxysilane. Briefly, the process involves the reaction of titanium (IV) butoxide with partially polymerized alkoxysilane, followed by hydrolytic polycondensation leading to gel formation. The details of procedures to prepare the solutions are given in Table 5. Transparent gels were obtained from all polymeric solutions.

Drying of Gels and Gel Monoliths

Gels and gel monoliths were dried by adopting two different techniques:

- Drying in air
- Supercritical drying.

Drying in air was performed under either infrared lamp or in an air oven at approximately 70 C for several days.

Supercritical drying was performed in an autoclave. The temperature of the sample was gradually raised above the critical temperature of the solvent, followed by removal of the volatiles (moisture and solvent vapor) isothermally. In this technique, the pressure and temperature are raised until the liquid residing in the pore capillaries on the monoliths becomes a supercritical fluid at which point it is removed, thus avoiding large

TABLE 4. GEL PREPARATION PARAMETERS (GeO₂-PbO SYSTEM)

Gel Composition Composition Number	Composition		Starting Chemicals	Molar Ratios		Condition of Hydrolysis		pH After Hydrolysis.	Final Concentration (g/l)	Gelation Time at Ambient Temperature (hr)		
	Mol PbO	Percent GeO ₂		Catalyst Ge(OC ₂ H ₅) ₄	Water Ge(OC ₂ H ₅) ₄	Alcohol Ge(OC ₂ H ₅) ₄	Temp. (C)				Duration (Min)	
PG1 (a)	10	90	Ge(OC ₂ H ₅) ₄ (CH ₃ COO) ₂ Pb·Pb(OH) ₂	0.014 HNO ₃	0.0	33.8	-10	30*	1-2	~3	50	<120
PG1 (b)	10	90	Ge(OC ₂ H ₅) ₄ (CH ₃ COO) ₂ Pb·Pb(OH) ₂	0.014 HNO ₃	1.0	33.8	-10	30	1-2	3-4	50	<96
PG1 (c)	10	90	Ge(OC ₂ H ₅) ₄ (CH ₃ COO) ₂ Pb·Pb(OH) ₂	0.014 HNO ₃	2.0	33.8	-10	30	1-2	~3	50	~0.08
PG2 (a)	33	67	Ge(OC ₂ H ₅) ₄ (CH ₃ COO) ₂ Pb·Pb(OH) ₂	0.019 HNO ₃	0.0	47.7	-10	30*	1-2	~4	50	<90
PG2 (b)	33	67	Ge(OC ₂ H ₅) ₄ (CH ₃ COO) ₂ Pb·Pb(OH) ₂	0.019 HNO ₃	1.0	38.2	-10	30	1-2	~4	62	<72
PG3 (a)	50	50	Ge(OC ₂ H ₅) ₄ (CH ₃ COO) ₂ Pb·Pb(OH) ₂	0.03 HNO ₃	0.0	72.9	-10	30*	~1	~5	50	<65
PG3 (b)	50	50	Ge(OC ₂ H ₅) ₄ (CH ₃ COO) ₂ Pb·Pb(OH) ₂	0.03 HNO ₃	1.0	57.5	-10	30	~1	4-5	60	<18

* Mixing time.

TABLE 5. GEL PREPARATION PARAMETERS (SiO₂-TiO₂ SYSTEM)

Serial Number	Starting Chemicals	Catalyst		Molar Ratios		Condition of Hydrolysis		pH After Hydrolysis	Reaction with Ti(Si ₂ O ₇) ₄		Solution Concentration (g/l)	
		Alkoxy silane	Water	Alkoxy silane	Alcohol Alkoxy silane	Temp. (C)	Duration (Hr)		Reaction Time (Hr)	Reaction Temp (C)		pH
1	Si(OC ₂ H ₅) ₄	0.03		2 (1)*	11.5 C ₂ H ₅ OH	40	3	<2	2	Ambient	<2	30
	Ti(OC ₄ H ₉) ₄	HCl			6.1 C ₄ H ₉ OH							
2	Si(OC ₂ H ₅) ₄	0.03	HCl	2 (1)	11.5 C ₂ H ₅ OH	40	3	<2	2	Ambient	<2	30
	Ti(OC ₄ H ₉) ₄	.001	HF		6.1 C ₂ H ₉ OH							
3	Si(OC ₂ H ₅) ₄	0.03		2 (1)	11.5 C ₂ H ₅ OH	40	1	<2	2	Ambient	<2	30
	Ti(OC ₄ H ₉) ₄	HCl			6.1 C ₄ H ₉ OH							
4	Si(OC ₂ H ₅) ₄	0.03		4 (1)	11.5 C ₂ H ₅ OH	40	1	<2	2	Ambient	<2	30
	Ti(OC ₄ H ₉) ₄	HCl			6.1 C ₄ H ₉ OH							
5	Si(OC ₂ H ₅) ₄	0.003		2 (1)	11.5 C ₂ H ₅ OH	40	1	<2	2	Ambient	-3	30
	Ti(OC ₄ H ₉) ₄	HCl			6.1 C ₄ H ₉ OH							
6	Si(OC ₂ H ₅) ₄	0.003		4 (1)	11.5 C ₂ H ₅ OH	40	1	<2	2	Ambient	-3	30
	Ti(OC ₄ H ₉) ₄	HCl			6.1 C ₄ H ₉ OH							
7	Si(OCH ₃) ₄	0.03		2 (1)	22.7 CH ₃ OH	Ambient	2	<2	2	Ambient	2	30
	Ti(OC ₄ H ₉) ₄	HCl			8.7 C ₂ H ₅ OH							
8	Si(OCH ₃) ₄	0.03		4 (1)	22.7 CH ₃ OH	Ambient	2	<2	2	Ambient	<2	30
	Ti(OC ₄ H ₉) ₄	HCl			8.7 C ₂ H ₅ OH							
9	Si(OCH ₃) ₄	0.003		2 (1)	22.7 CH ₃ OH	Ambient	2	<2	2	Ambient	3-4	30
	Ti(OC ₄ H ₉) ₄	HCl			8.7 C ₂ H ₅ OH							
10	Si(OCH ₃) ₄	0.003		4 (1)	22.7 CH ₃ OH	Ambient	2	<2	2	Ambient	3-4	30
	Ti(OC ₄ H ₉) ₄	HCl			8.7 C ₂ H ₅ OH							

* The figures within parentheses represent the molar ratio used for initial hydrolysis of alkoxy silane.

capillary pressures associated with liquid-solid surface tension during slow evaporation of solvent at room temperature. Figure 1 shows a schematic diagram of the arrangements for supercritical drying of gel monoliths.

Characterization of Gels

The following physicochemical aspects of the gels were characterized:

- Homogeneity of microstructures by scanning electron microscopy
- Molecular structures of as-prepared and thermally treated gels by infrared spectroscopy
- Crystallization tendency of gels by the DTA and X-ray powder diffraction techniques.

SiO₂-GeO₂ System. After thermal treatment up to 500 C, gels were examined by differential thermal analysis, X-ray diffraction technique, and infrared spectroscopy. X-ray diffraction (XRD) studies indicated that compositions with GeO₂ up to 15 percent were noncrystalline; however, crystallinity was detected with compositions having 20 percent GeO₂. Differential thermal analysis and infrared spectroscopic analysis of different samples are continuing and will be discussed in the next report.

Differential Thermal Analysis. Differential thermal analyses have been performed with SG 1, SG 2, SG 5, and SG 6 gels up to 1300 C at the heating rate of 10 C/min in an oxygen atmosphere. The DTA curves are shown in Figures 2 to 5. Observe that except SG 1 all other composition gels show tendency to crystallization in the range of 800 to 1200 C. However, XRD of the samples need to be performed to confirm the DTA results.

Infrared Spectroscopic Studies. Infrared spectroscopic analyses of air-dried gels in the SiO₂-GeO₂ system were performed to examine their molecular structures. Also, infrared spectra of autoclaved gels were obtained to study the influence of drying technique on the molecular structure. The results are being examined and will be reported later. X-ray diffraction

ORIGINAL PAGE IS
OF POOR QUALITY

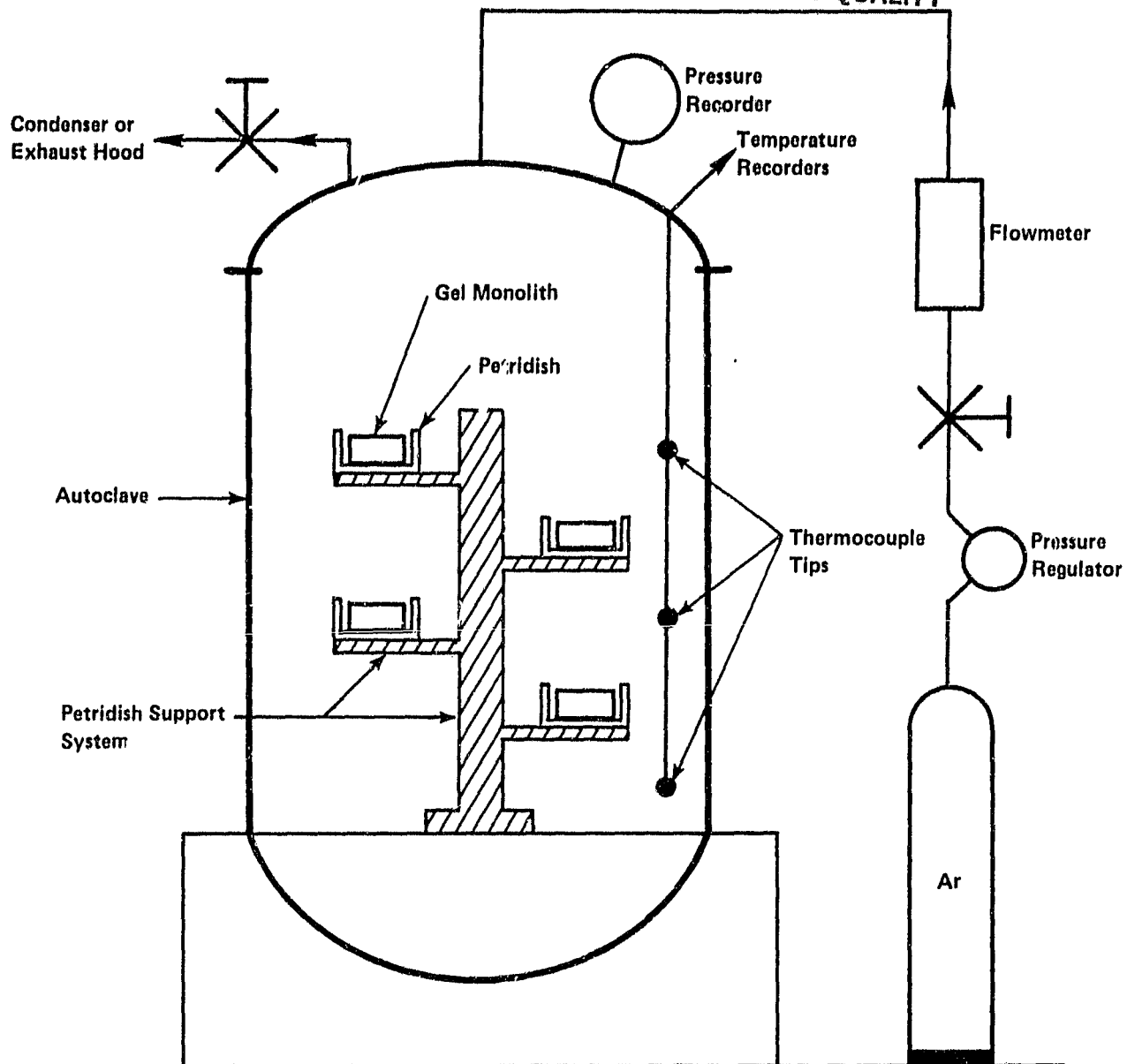


FIGURE 1. SCHEMATIC DIAGRAM SHOWING THE ARRANGEMENTS FOR SUPERCRITICAL DRYING OF GEL MONOLITH. PROGRAM CONTROLLER AND THE HEATING SYSTEM ARE NOT SHOWN.

ORIGINAL PAGE IS
OF POOR QUALITY

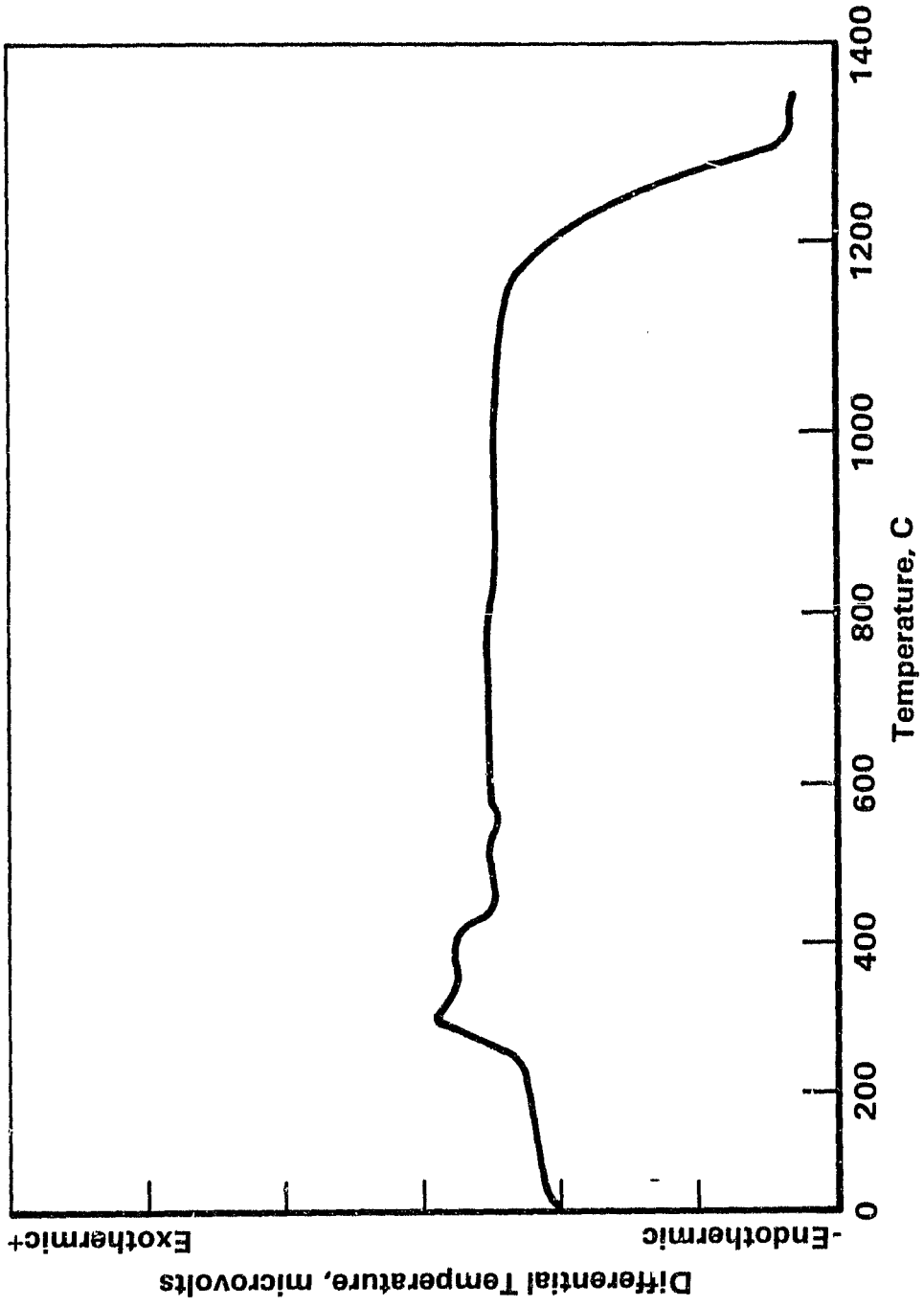


FIGURE 2. DIFFERENTIAL THERMAL ANALYSIS OF SG 1 GEL

ORIGINAL PAGE IS
OF POOR QUALITY

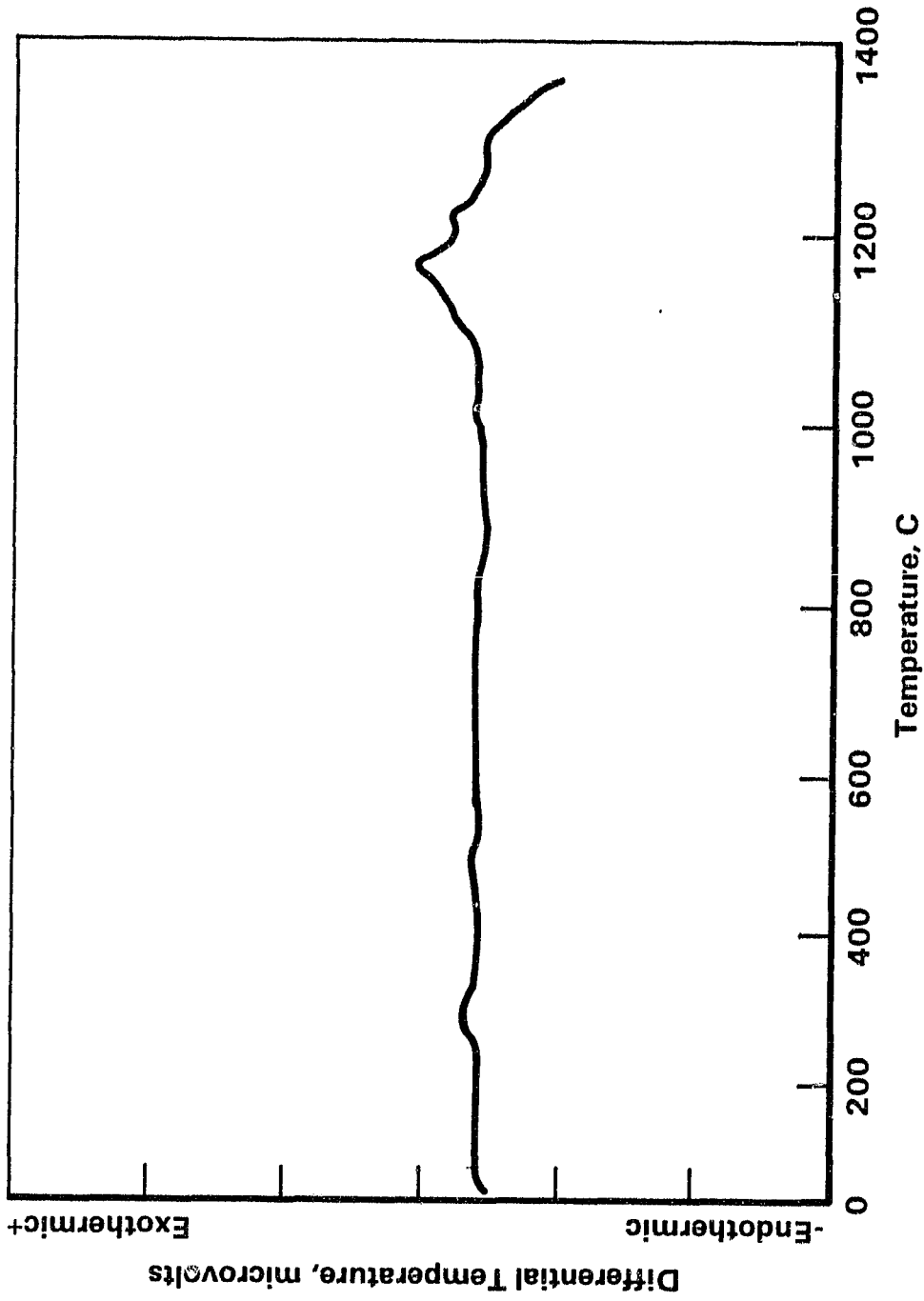


FIGURE 3. DIFFERENTIAL THERMAL ANALYSIS OF SG 2 GEL

ORIGINAL PAGE IS
OF POOR QUALITY

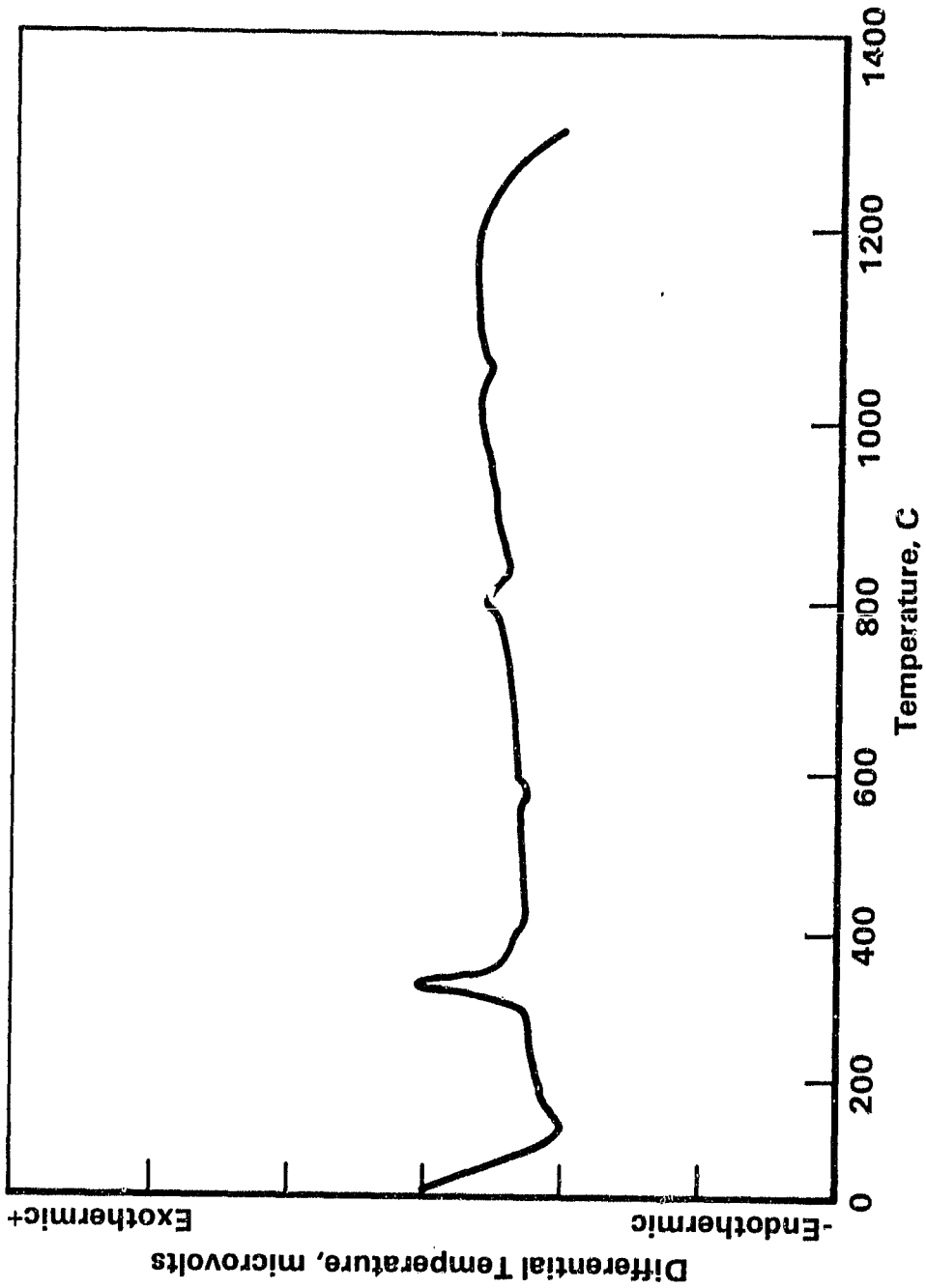


FIGURE 4. DIFFERENTIAL THERMAL ANALYSIS OF SG 5 GEL

ORIGINAL PAGE IS
OF POOR QUALITY

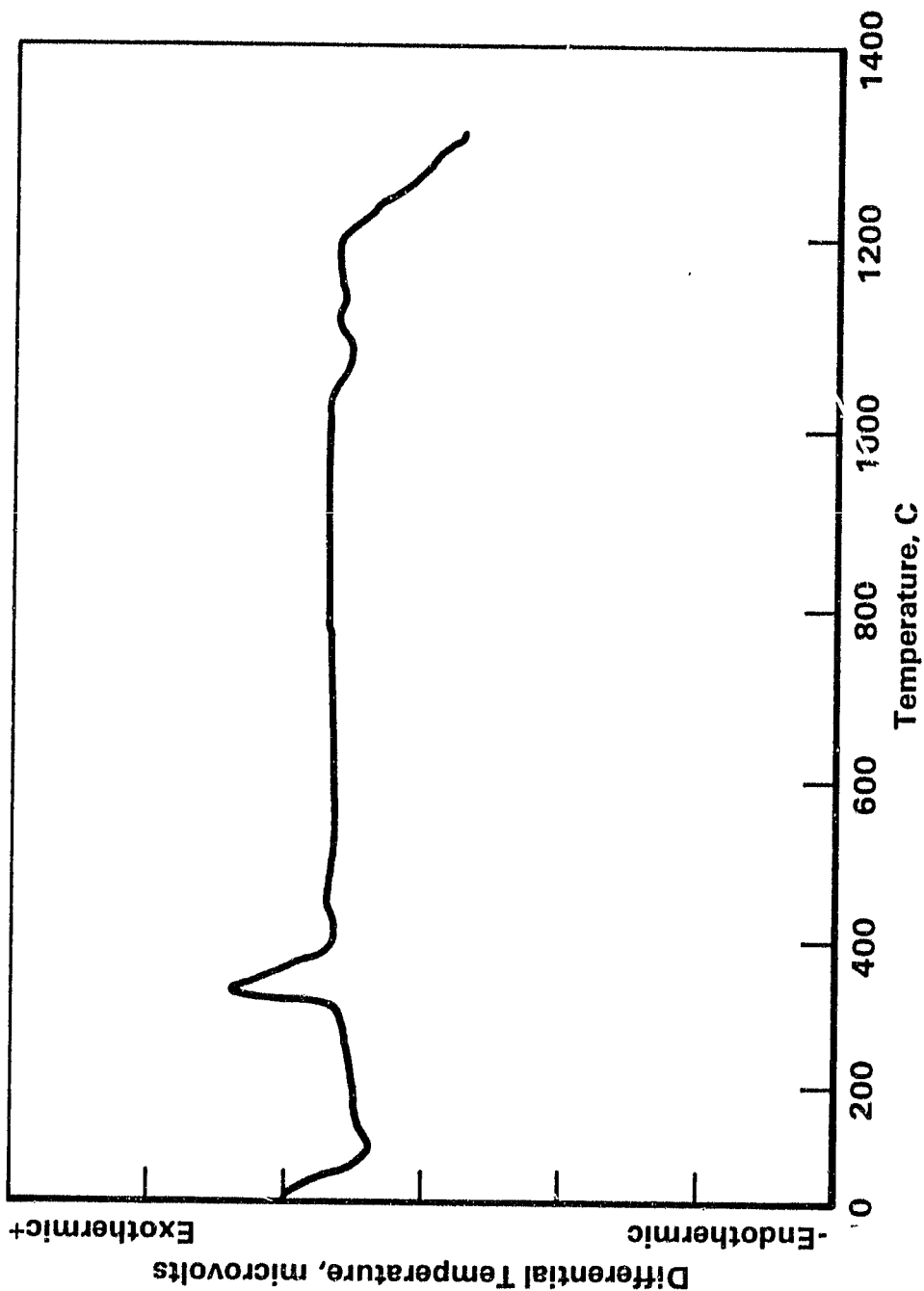


FIGURE 5. DIFFERENTIAL THERMAL ANALYSIS OF SG 6 GEL

analyses by the powder method were performed on selected gel samples after different thermal treatments. The results are shown in Table 6.

GeO₂-PbO System. The following physicochemical aspects of the gels were characterized.

Homogeneity. After drying at 70 C for several days, as-prepared PG 1(b) gel was examined by scanning electron microscopy to determine the microstructural homogeneity of the gel in terms of particle size, particle-size distribution, and pore morphology. Figure 6 shows the scanning electron photomicrograph of the as-prepared gel dried at 70 C. Observe that the gel structure consists of particles in the size range of approximately 200 to 500 Å.

Molecular Structure. The molecular structures of as-prepared PG 1(a), PG 1 (b), PG 1(c), PG 2(b), and PG 3(b) gels after drying at 70 C were examined by infrared spectroscopy. The IR spectra of the above gels are shown in Figures 7 to 11. The IR spectrum of the supercritically dried PG 1(c) gel is shown in Figure 12. The spectra were taken by the KBr pellet method. The infrared absorption peaks/bands of the gels are listed in Table 7. The infrared spectra of lead acetate, lead oxide, and germanium dioxide (amorphous and crystalline) are shown in Figures 13-16, and the absorption peaks/bands are listed in Table 8.

Observe that in PG 1(a) gel (Figure 7) the absorption peak due to main O-Ge-O assymmetric stretching vibration occurs at 830 cm⁻¹ which is the same as for PG 1(b) gel (Figure 8). Moreover, both PG 1(a) and PG 1(b) gels show absorption peaks at 550 cm⁻¹ resulting from symmetrical O-Ge-O bending-stretching vibration mode. Obviously, both PG 1(a) and PG 1(b) are structurally very similar and the coordination characteristics of these gels (between GeO₄ unit and Pb⁺² ion) are similar to those of GeO₂-PbO glass. PG 1(c) gel (Figure 9) shows absorptions due to assymmetric O-Ge-O stretching vibrations at 880 cm⁻¹ and 760 cm⁻¹, and overlapping peaks at 580 cm⁻¹, 540 cm⁻¹, and 520 cm⁻¹ due to symmetrical O-Ge-O bending-stretching vibrations. The absorption characteristic is similar to that exhibited by crystalline GeO₂. As shown

TABLE 6. RESULTS OF X-RAY POWDER DIFFRACTION PATTERNS

Composition	Starting Compounds	Final pH	Catalyst	Drying Condition Atmosphere	Temperature (C)	Crystallinity
SG 1	Si(OC ₂ H ₅) ₄	2-3	HF	Air	500	Noncrystalline
SG 2	(a) Si(OC ₂ H ₅) ₄	2-3	HCl	Autoclaved		Noncrystalline
	(b) Si(OCH ₃) ₄	6-7	NH ₄ OH	Autoclaved		Noncrystalline
SG 4	Si(OC ₂ H ₅) ₄	<2	HCl	Air	70	Crystalline
SG 5	Si(OCH ₃) ₄	<2	HCl	Air	70	Noncrystalline
SG 6	Si(OCH ₃) ₄	<2	HCl	Air	600	Noncrystalline
	Ge(OC ₂ H ₅) ₄			Air	70	Noncrystalline

ORIGINAL PAGE IS
OF POOR QUALITY



1 cm = 0.19 μ

51,000X

FIGURE 6. SCANNING ELECTRON PHOTOMICROGRAPH OF
PG 1(b) GEL DRIED AT 70 C

ORIGINAL PAGE IS
OF POOR QUALITY

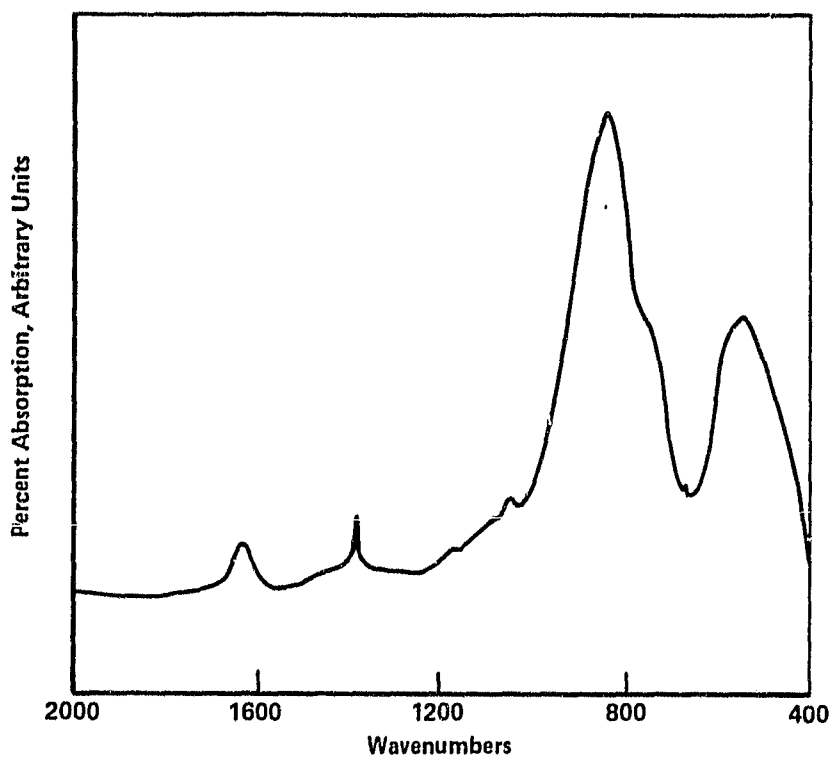


FIGURE 7. INFRARED SPECTRUM OF PG 1(a) GEL
DRIED AT 70 C

ORIGINAL QUALITY
OF POOR QUALITY

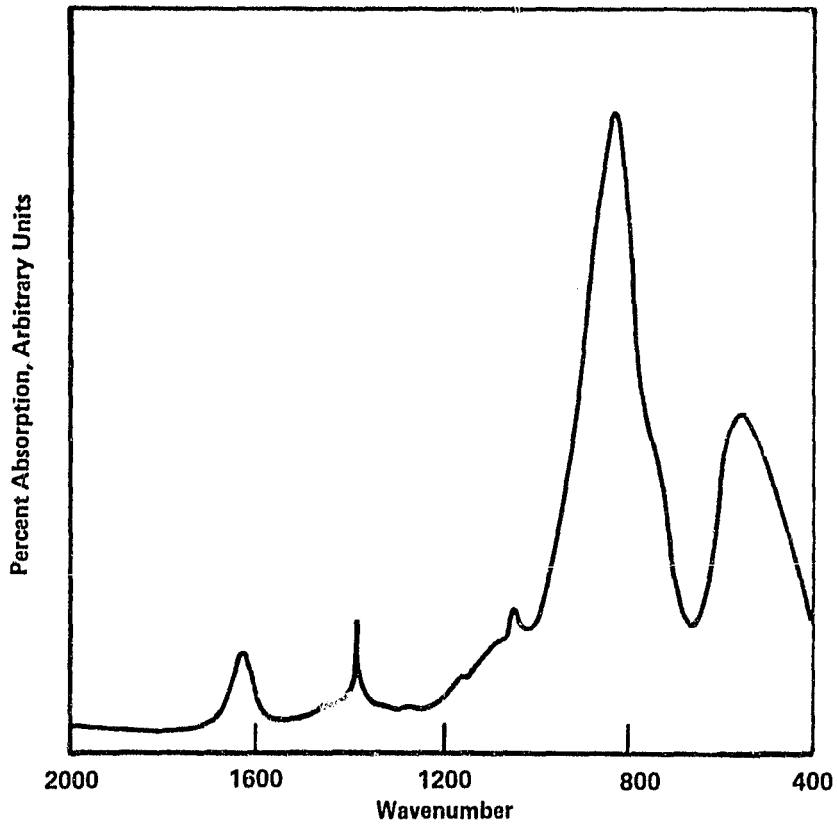


FIGURE 8. INFRARED SPECTRUM OF PG 1(b) GEL
DRIED AT 70 C

ORIGINAL PAGE IS
OF POOR QUALITY

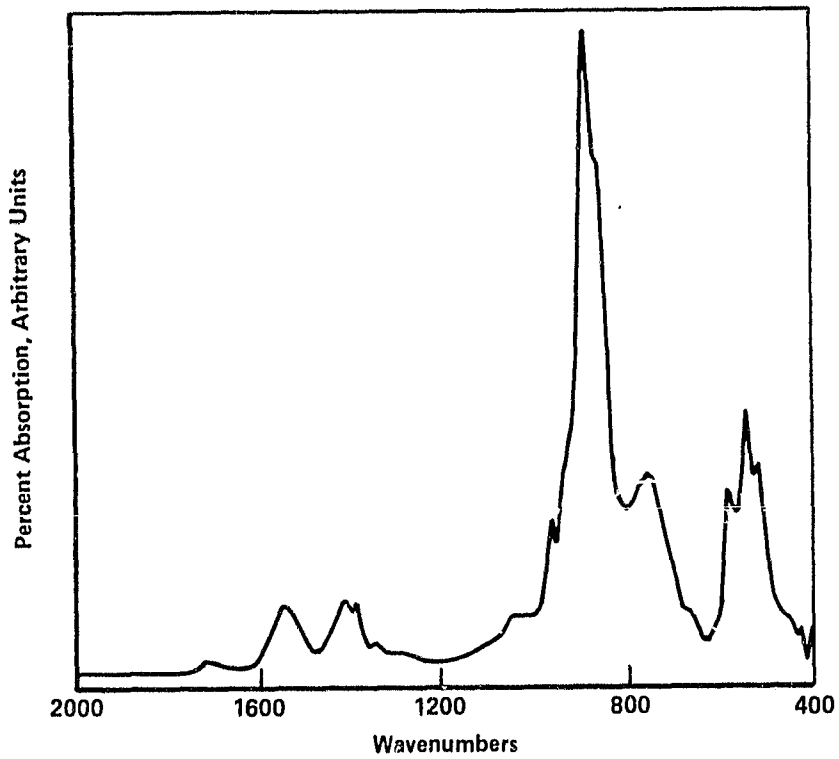


FIGURE 9. INFRARED SPECTRUM OF PG 1(c) GEL
DRIED AT 70 C

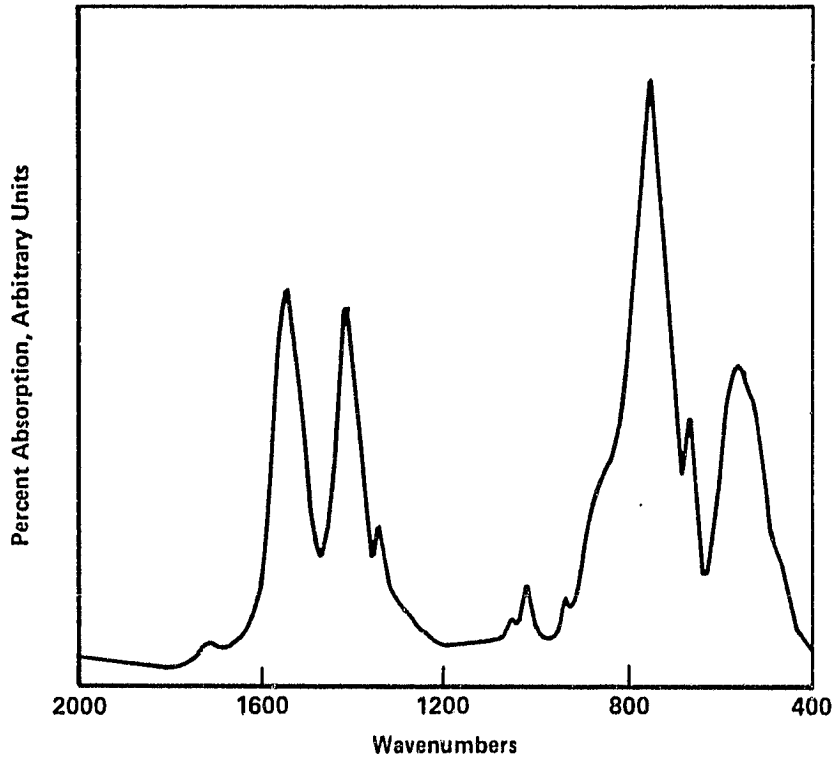


FIGURE 10. INFRARED SPECTRUM OF PG 2(b) GEL
DRIED AT 70 C

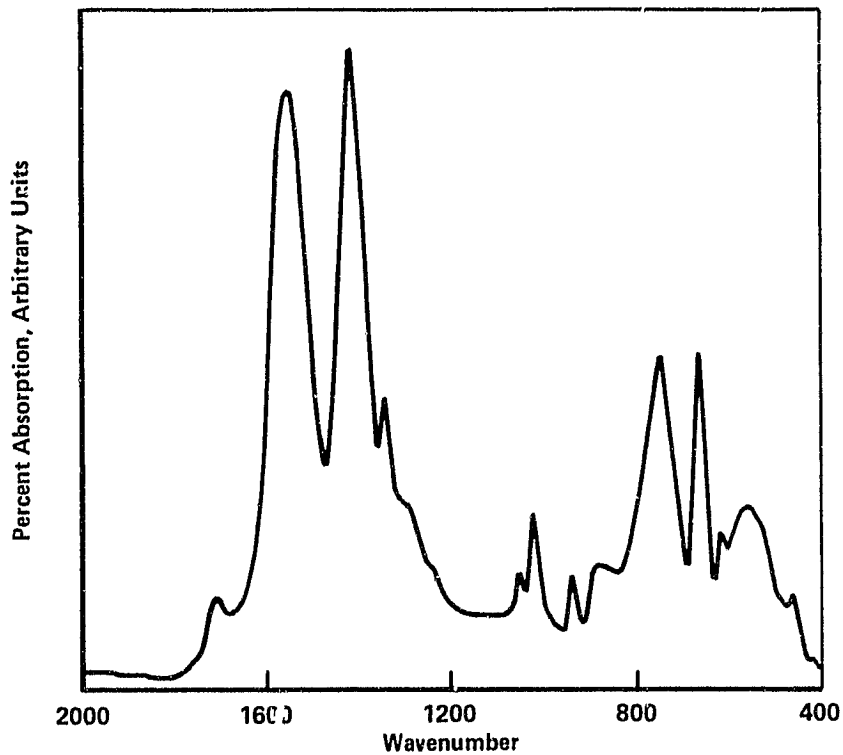


FIGURE 11. INFRARED SPECTRUM OF PG 3(b) GEL
DRIED AT 70 C

ORIGINAL PAGE IS
OF POOR QUALITY.

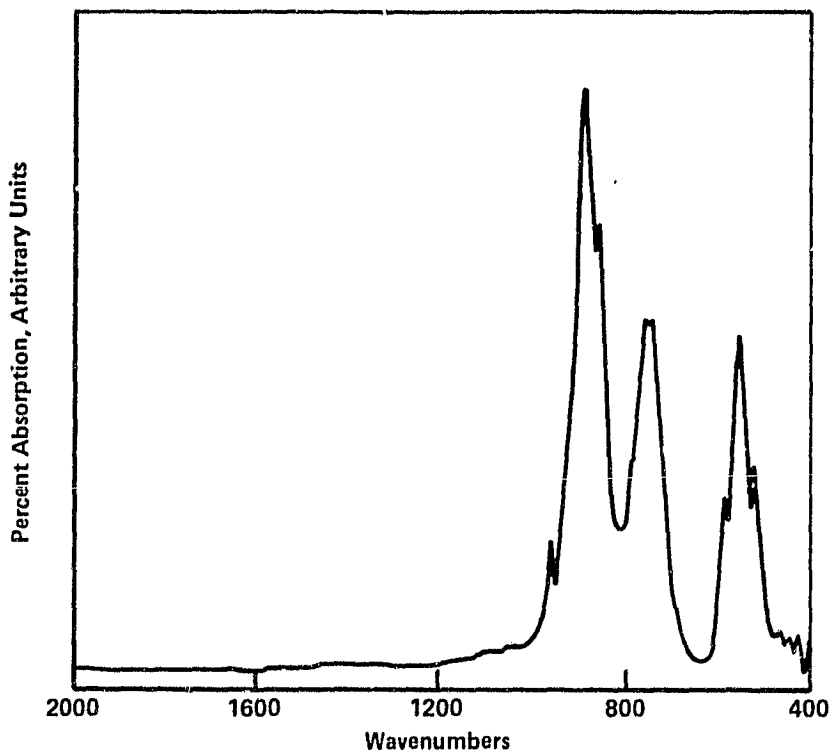


FIGURE 12. INFRARED SPECTRUM OF SUPERCRITICALLY
DRIED PG 1(c) GEL

TABLE 7. INFRARED ABSORPTION FREQUENCIES OF LEAD GERMANATE GELS

PG 1(a) Gel Dried at 70 C	PG 1(c) Gel Dried at 70 C	PG 1(c) Gel Supercritically Dried	PG 2(b) Gel Dried at 70 C	PG 3(b) Gel Dried at 70 C
			1710 V.V. Small peak, broad	1710 V. Small peak, broad
1630 V.V. Small peak, broad			1540 Large peak, sharp	1550 V. Large peak, sharp
	1540 Small peak, broad		1410 Large peak, sharp	1410 V. Large peak, sharp
	1410 Small peak, broad		1340 Small peak, sharp	1340 Small peak, sharp
1390 Small peak, sharp	1380 Small peak, sharp		1020 V. Small peak, sharp	1020 Small peak, sharp
			940 V.V. Small peak, broad	940 V. Small peak, sharp
	880 V. Large peak, sharp	880 V. Large peak, sharp		
	860 Submerged peak, sharp	860 Submerged peak, sharp		
830 V. Large peak, sharp				
750 Large over- lapping peak	760 Small peak, broad	750-740 Large peak, sharp	750 V. Large peak, sharp	750 Large peak, sharp
			670 Large peak, sharp	660 Large peak, sharp
	580 Small peak, sharp	580 Small peak, sharp		
			560 Large peak, sharp	560 Small peak broad
550 Large peak, broad	540 Large peak, sharp	540 Large peak, sharp		
	520 Small peak, sharp	520 Small peak, sharp		

ORIGINAL PAGE IS
OF POOR QUALITY

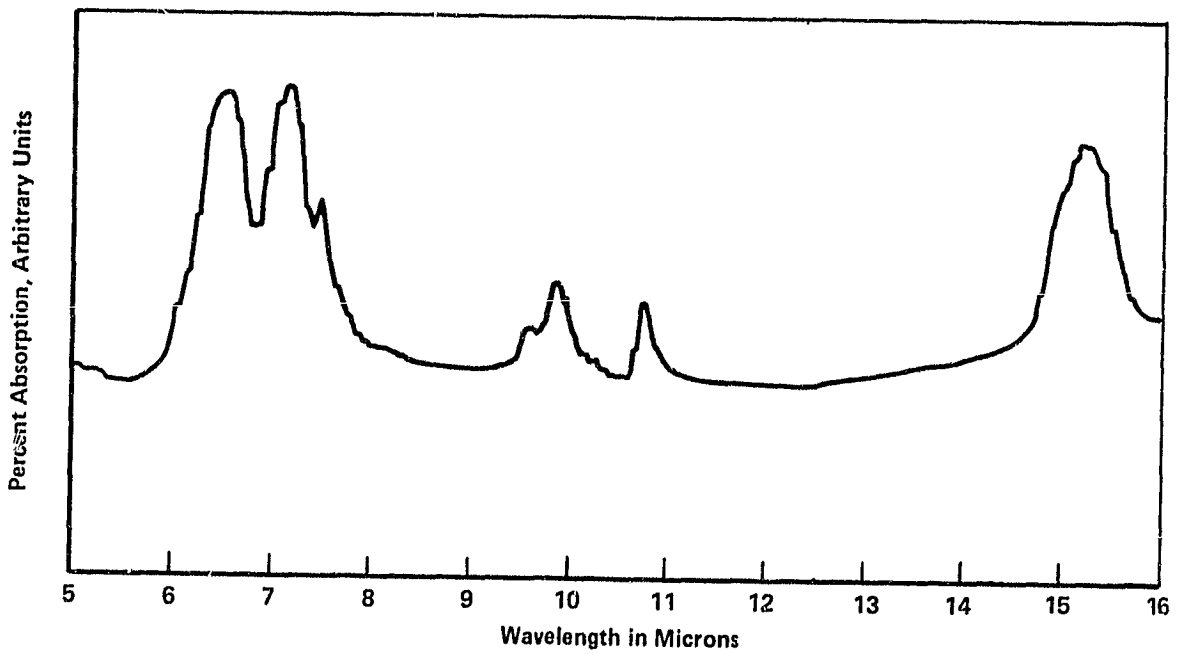
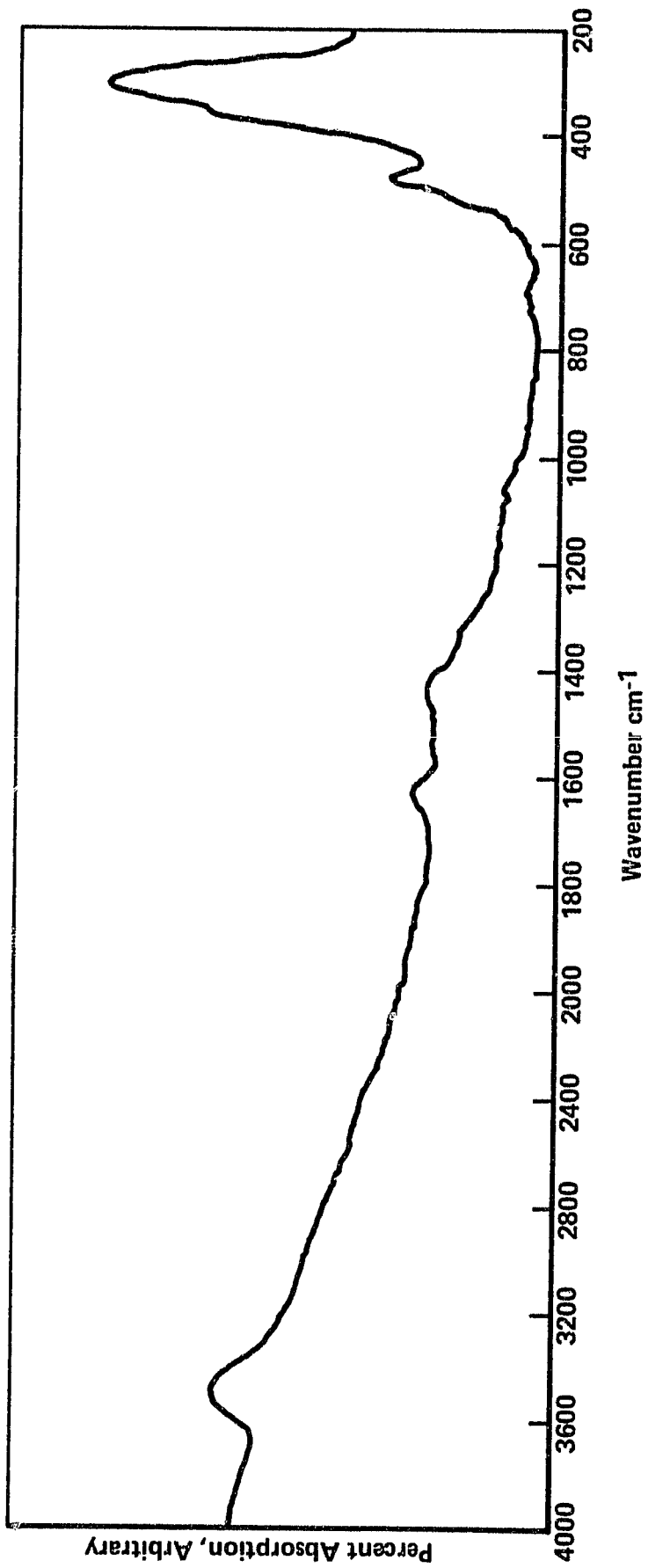


FIGURE 13. INFRARED SPECTRUM OF LEAD ACETATE TRIHYDRATE



ORIGINAL PAGE IS
OF POOR QUALITY

FIGURE 14. INFRARED SPECTRUM OF LEAD OXIDE (PbO)

ORIGINAL PAGE IS
OF POOR QUALITY

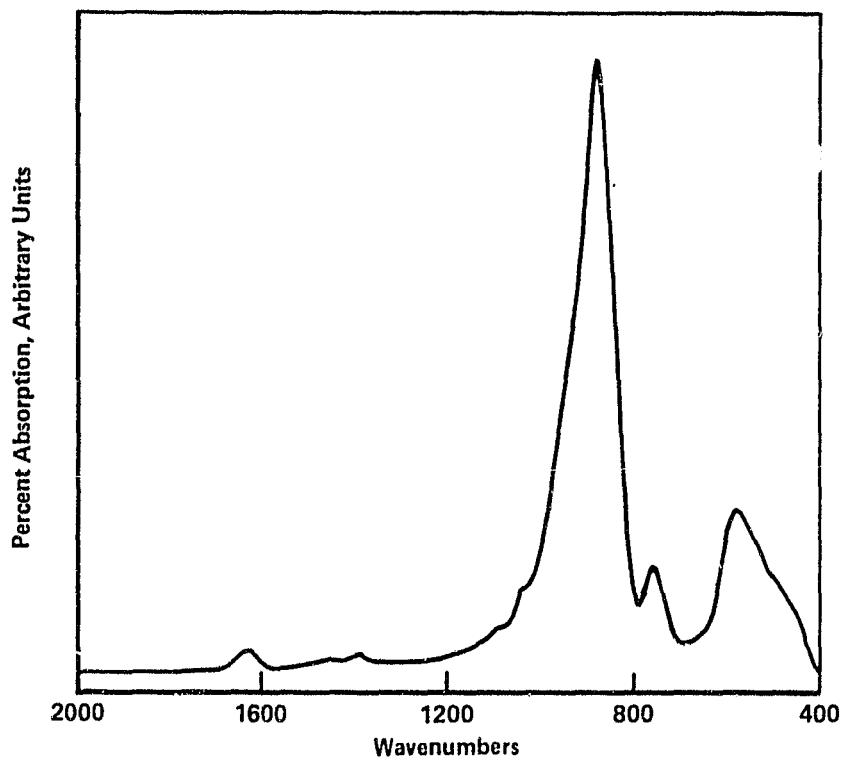


FIGURE 15. INFRARED SPECTRUM OF NONCRYSTALLINE
GERMANIUM OXIDE

ORIGINAL PAGE IS
OF POOR QUALITY

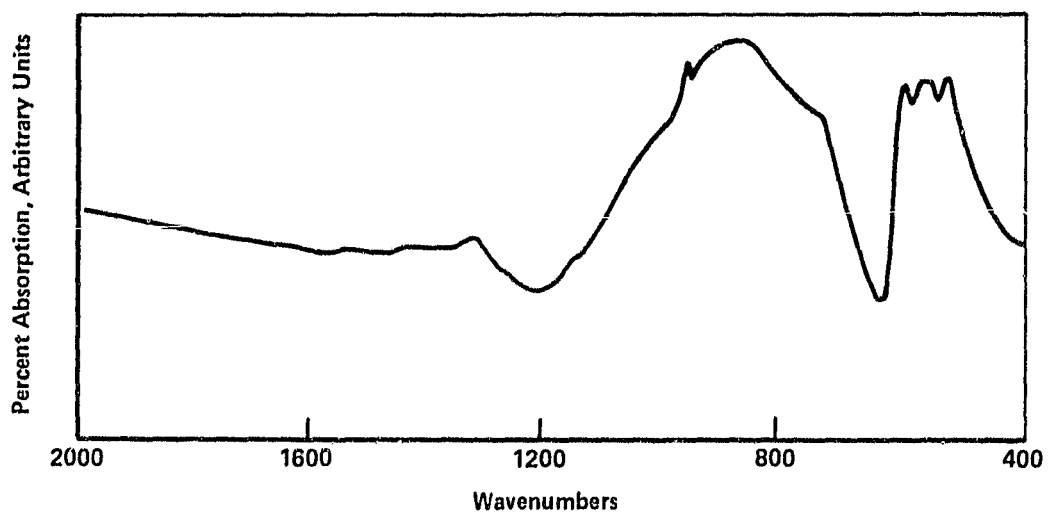


FIGURE 16. INFRARED SPECTRUM OF CRYSTALLINE GERMANIUM OXIDE

TABLE 8. INFRARED ABSORPTION FREQUENCIES OF LEAD ACETATE, LEAD OXIDE, AND GERMANIUM OXIDE (FREQUENCY RANGE 4000 to 400 cm^{-1})

$\text{Pb}(\text{OOCCH}_3)_2 \cdot 3\text{H}_2\text{O}$	$\text{Pb}(\text{OOCCH}_3)_4$	PbO	Noncrystalline GeO_2 GeI	Crystalline GeO_2
		~1620 V.V.S peak, broad	1630 V.V.S peak, broad	
~1540 Large peak, sharp	~1540 Large peak, sharp			
~1400 Large peak, sharp	~1430 Large peak, sharp			
~1333 Small peak, sharp			~1390 V.V. small peak, broad	~1320 V.V. small peak, broad
~1050 V. Small broad	~1050 Small peak, sharp			
~1010-1015 Small, sharp	~1020 Small peak, sharp			
~930 Small peak, sharp				
			880 V. Large peak, sharp	870 V. Large peak, V. broad
	~700 Large peak, sharp		750 Small peak, broad	720 Large over- lapping peak
~660 Large peak, sharp				
	630 Large peak, sharp			
			570 Large peak, broad	580, 550, and 520 overlapping peaks
		480 Small peaks, sharp		

later, the X-ray diffraction analysis of this gel (dried at 70 C) indicates the presence of partially crystalline GeO_2 . Moreover, observe that a sharp peak is present at 860 cm^{-1} frequency (overlapped with the peak at 880 cm^{-1}). We have assumed that this absorption peak at slightly lower frequency results from the asymmetric O-Ge-O stretching vibration in the $\text{GeO}_2\text{-PbO}$ gel structure (due to the ionic interaction of the bond between GeO_4 unit and Pb^{+2} ion). Thus, the PG 1(c) gel structure is characterized by a shift of the main O-Ge-O asymmetric stretching vibration towards higher frequency than that observed in PG 1(a) and PG 1(b) gels. This indicates that the molecular structure of PG 1(c) gel is different from PG 1(a) and PG 1(b) gels. The difference in the molecular structure may be due to the preparation procedure. The absorption peaks at frequencies 1540 cm^{-1} , 1410 cm^{-1} , and 1380 cm^{-1} are similar to those exhibited by lead acetate trihydrate (Figure 13; Table 8). But lead acetate trihydrate shows a large absorption peak at 660 cm^{-1} frequency absent in the IR spectrum of PG 1(c) gel. This may be because discrete (unreacted) lead acetate molecules were not present in the gel. Perhaps a small fraction of lead acetate molecules were bonded to GeO_4 units somewhat differently. This phenomenon may be due to the distance and the force constant between GeO_4 unit and lead acetate molecule. Note that X-ray diffraction analyses of this gel do not show any peak or diffused band corresponding to lead acetate. The IR spectrum of the supercritically dried PG 1(c) gel (Figure 12) is characterized by the absence of absorption peaks at 1540 cm^{-1} , 1410 cm^{-1} , and 1380 cm^{-1} frequencies, showing that the molecular structures changed during supercritical drying. The profiles of the IR peaks of PG 2(b) and PG 3(b) gels (Figures 10 and 11) were identical. A comparison of the peak positions in Figures 10 and 11 indicates that PG 2(b) and PG 3(b) gels are structurally similar, with some absorption peaks occurring due to the presence of lead acetate and germanium oxide. However, the absorption peak due to the main O-Ge-O asymmetric stretching mode was almost absent in both the gels. Instead, the secondary O-Ge-O asymmetric stretching mode of vibration at 750 cm^{-1} was predominant in both. It appears that the structures of PG 2(b) and PG 3(b) gels are very complex.

The following conclusions can be drawn from the IR studies:

- The gel structures depend on the preparation procedure and gel composition.
- The gel structures change on thermal treatment.

Crystallinity. The crystallization behaviors of the gels were studied by differential thermal analyses. Also, X-ray diffraction studies of the gels were made to identify the nature of crystallization. The samples studied are shown in Table 9.

TABLE 9. DESCRIPTION OF GELS STUDIED FOR THEIR CRYSTALLIZATION BEHAVIOR

Serial Number	Composition Number	Thermal Treatment (C)	Time	Remarks
1	PG 1(a)	70	Several days	--
2	PG 1(b)	70	Several days	--
3	PG 1(b)	500	30 min	--
4	PG 1(b)	600	30 min	--
5	PG 1(b)	1000		Sample obtained after DTA up to 1000 C
6	PG 1(c)	As-prepared		--
7	PG 1(c)	70	Several days	--
8	PG 1(c)	Supercritically dried		--
9	PG 2(b)	70	Several days	--
10	PG 3(b)	70	Several days	--

Differential Thermal Analysis--The differential thermal analysis of the gels were performed up to 1000/1100 C at the heating rate of 10 C/min in an oxidizing atmosphere. The DTA curves are shown in Figures 17-22. The position and nature of the DTA peaks are listed in Table 10. Differential thermal analyses were also performed on precipitated lead acetate (basic) and

ORIGINAL SAMPLES
OF POOR QUALITY

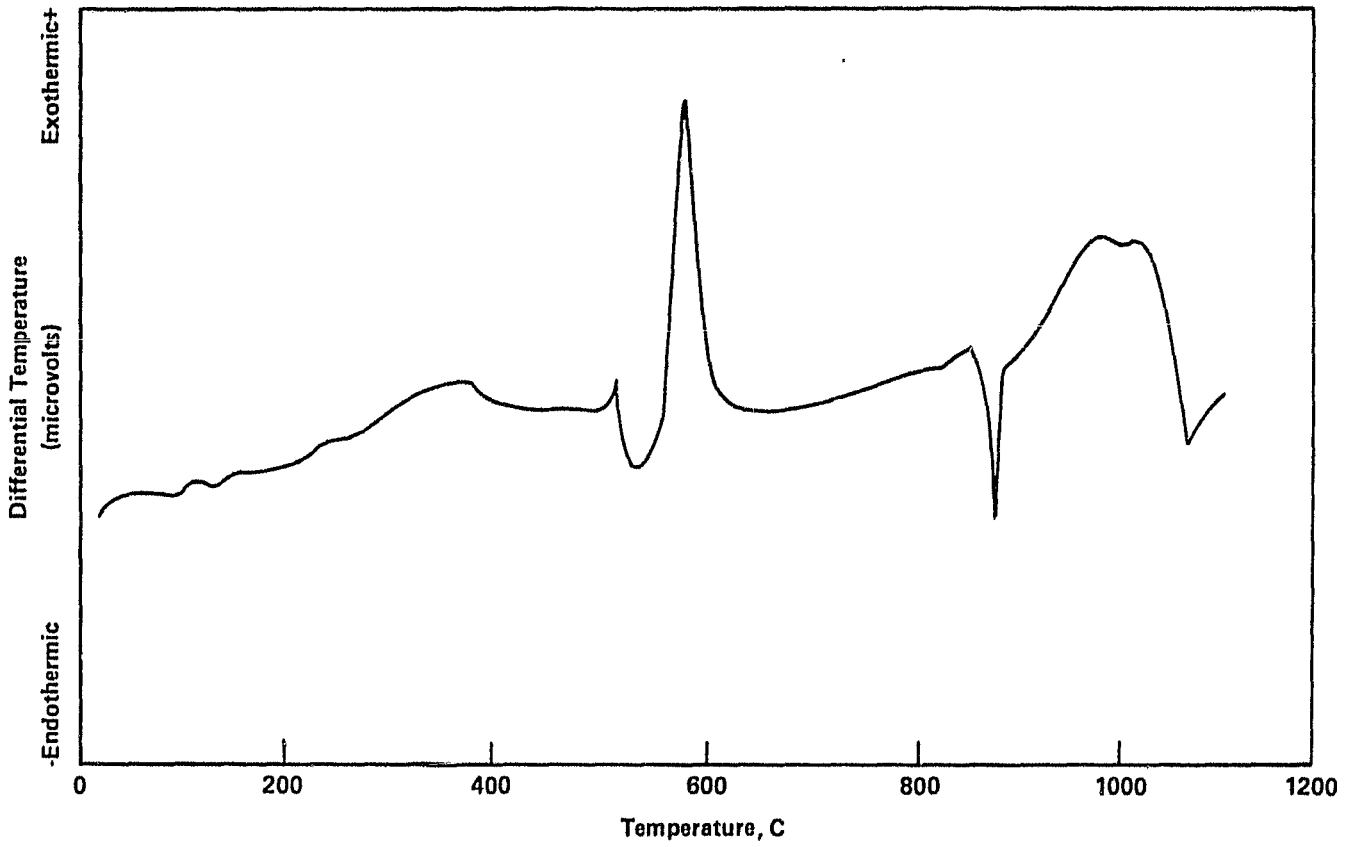


FIGURE 17. DIFFERENTIAL THERMAL ANALYSIS OF PG 1(a) GEL

ORIGINAL PAGE IS
OF POOR QUALITY

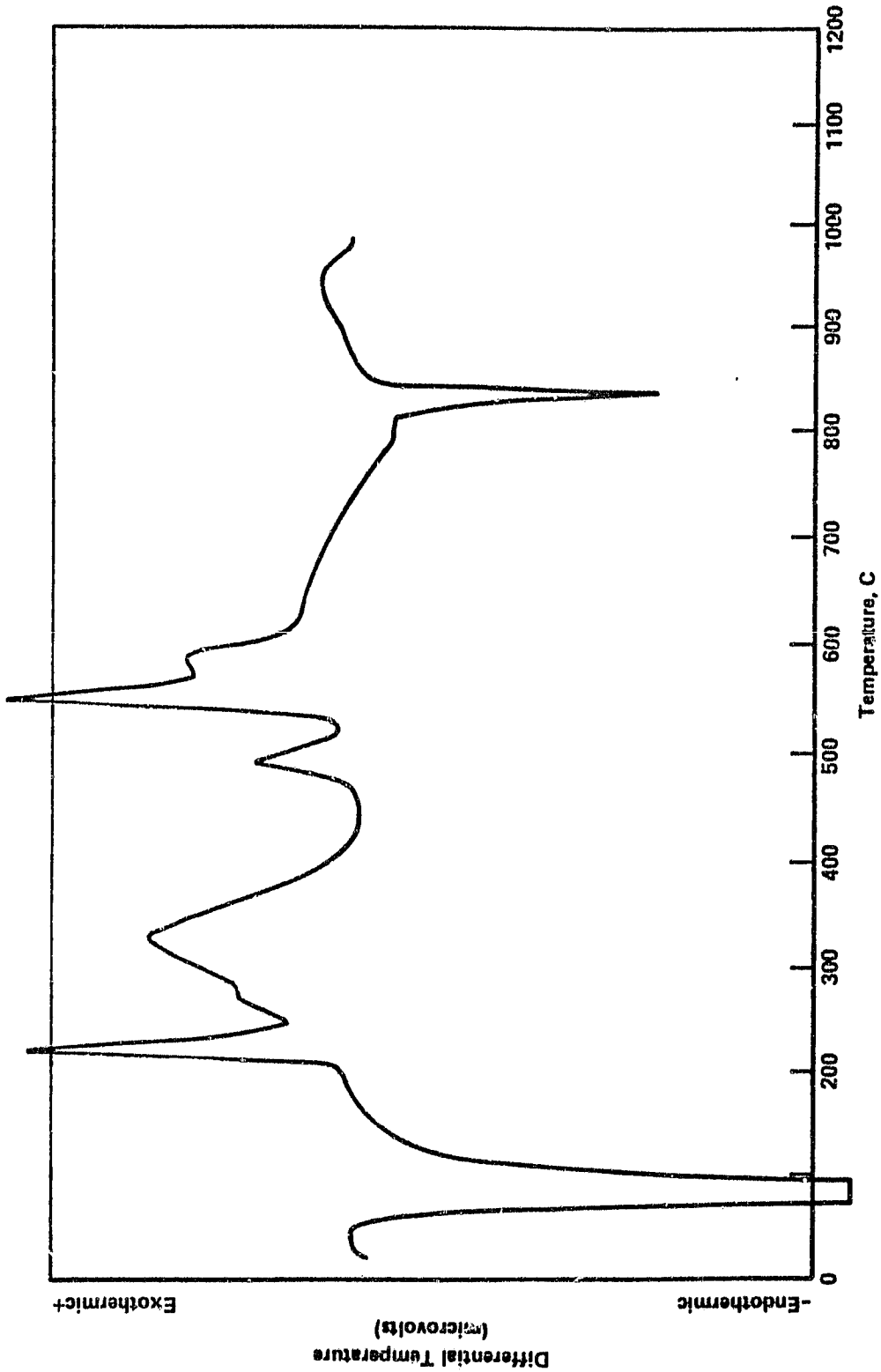


FIGURE 18. DIFFERENTIAL THERMAL ANALYSIS OF PG 1(b) GEL

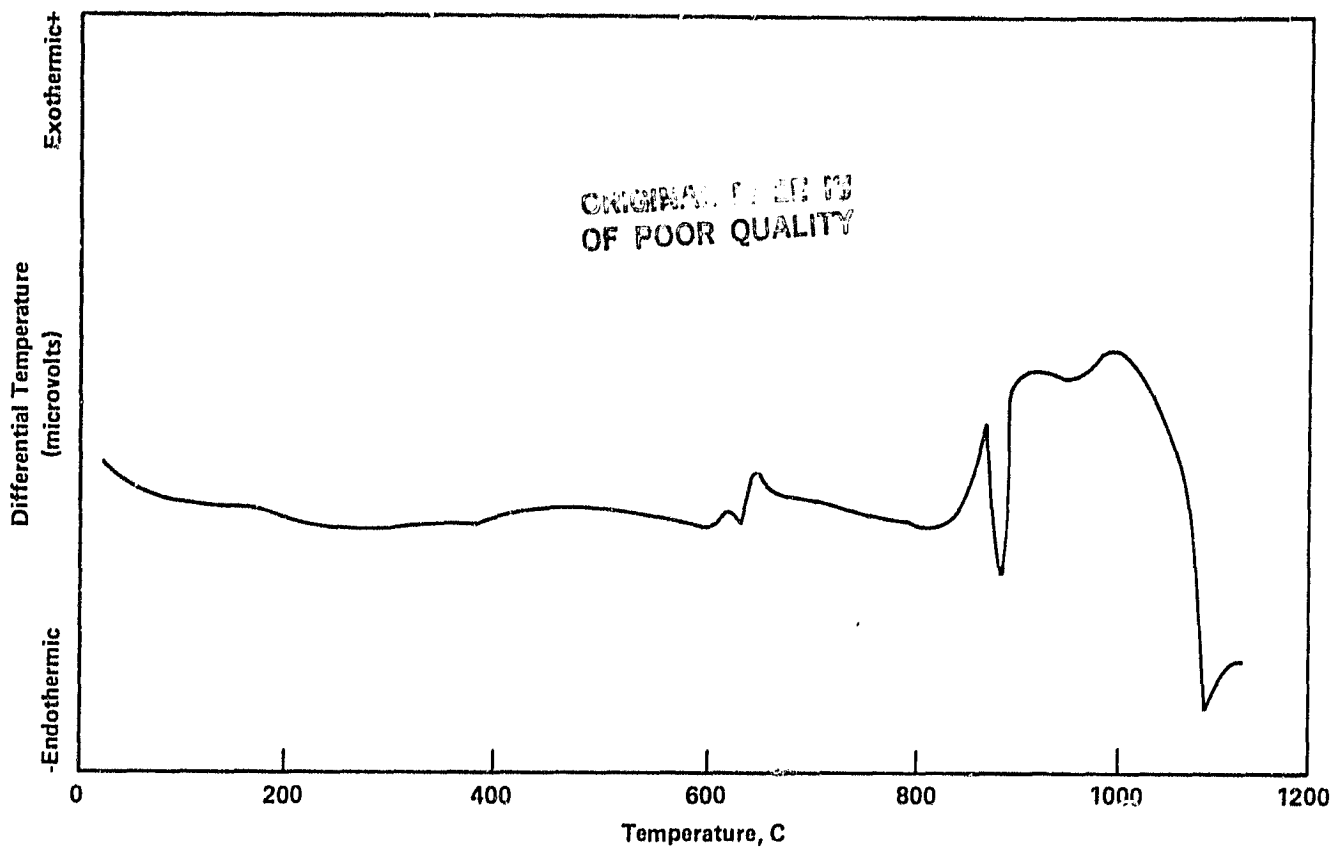


FIGURE 19. DIFFERENTIAL THERMAL ANALYSIS OF SUPERCRITICALLY DRIED PG 1(c) GEL

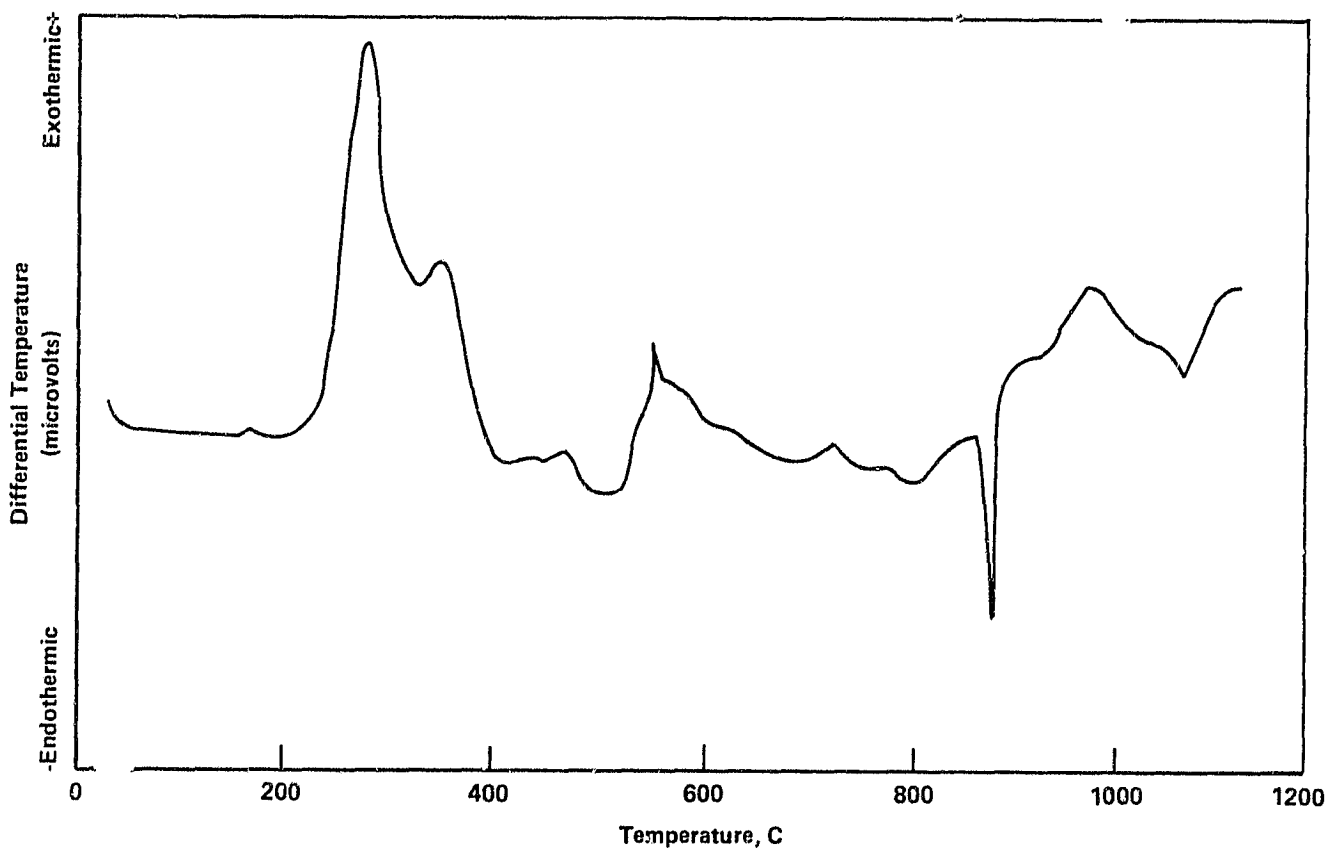


FIGURE 20. DIFFERENTIAL THERMAL ANALYSIS OF PG 1(c) GEL

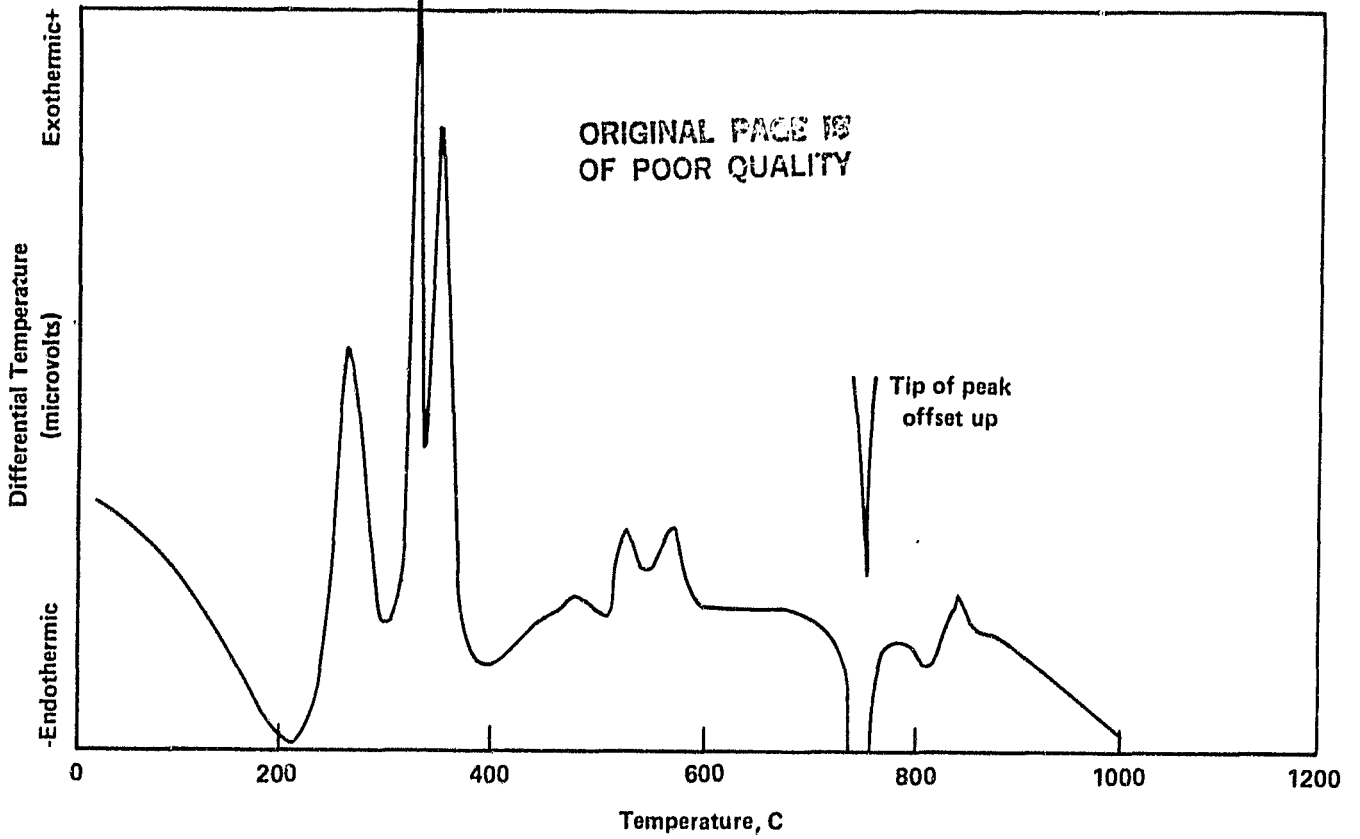


FIGURE 21. DIFFERENTIAL THERMAL ANALYSIS OF PG 2(b) GEL

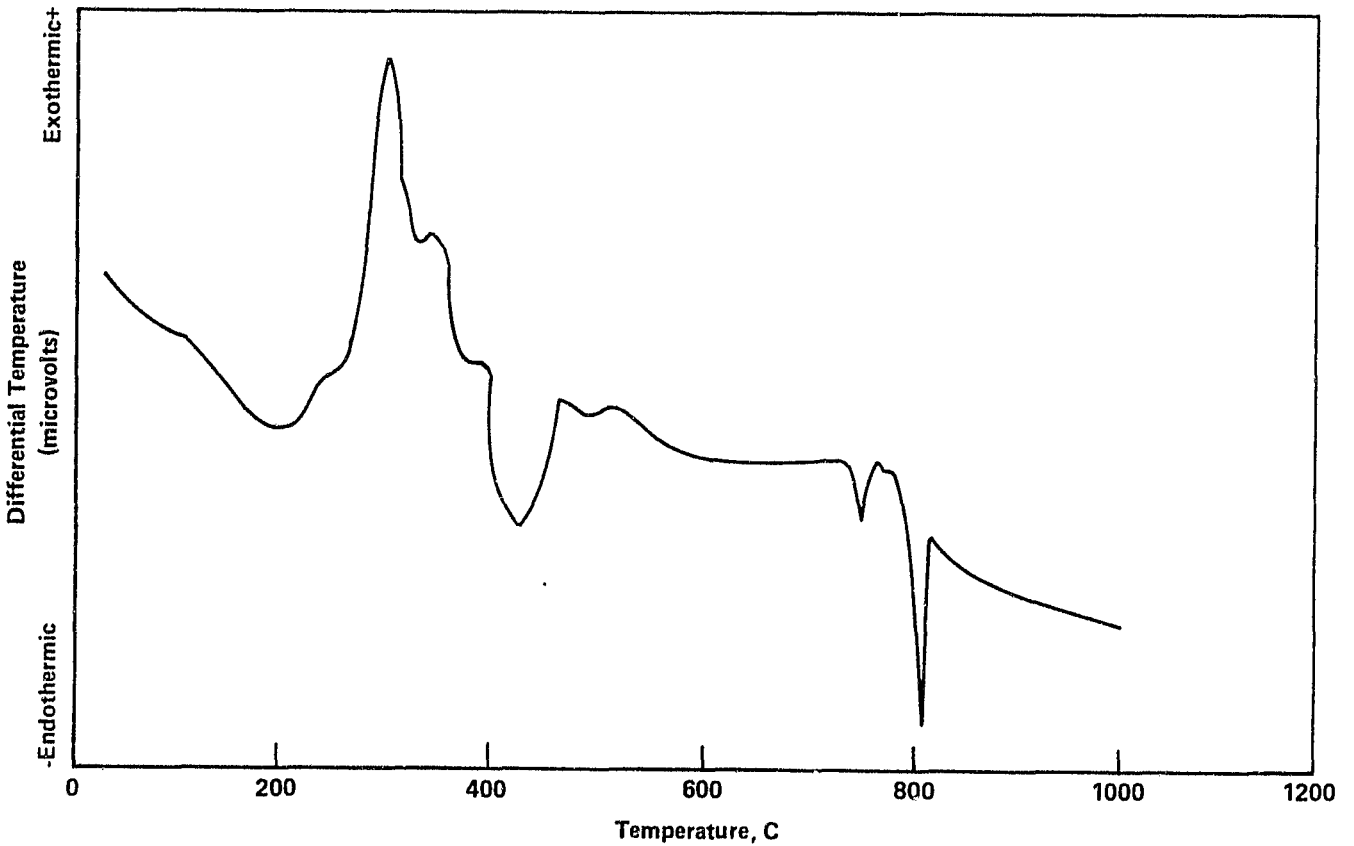


FIGURE 22. DIFFERENTIAL THERMAL ANALYSIS OF PG 3(b) GEL

TABLE 10. DTA PEAKS OF LEAD GERMANATE GELS

PG 1(a) Temperature (C)	PG 2(b) Gel Dried at 70 C Temperature (C)	PG 3(b) Gel Dried at 70 C Temperature (C)	PG 1(c) Gel Dried at 70 C Temperature (C)	PG 1(c) Gel Supercritically Dried Temperature (C)	PG 1(b) Gel Dried at 70 C Temperature (C)	Nature of Peaks
	220	200			85	Endo
	265	300	280		220	Exo
	330	345			330	Exo
	355		350			Exo
380	400	425	470			Endo
	485					Exo
510	530	465		450-500	490	Exo
		515	550			Exo Broad band
580	575		580		550	Exo
	755	750	625	620	585	Exo
			720	645		Exo
	815	805	775			Exo
850			860	870		Exo
875			875	885		Endo
970			970	990		Exo
1015			1070	1090		Endo
1070						Endo

noncrystalline germanium dioxide (prepared by partial hydrolysis of $\text{Ge}(\text{OC}_2\text{H}_5)_4$) at the identical heating rate for interpretation of the DTA results. The DTA curves are shown in Figures 23 and 24, respectively. The DTA of PG 1(a) gel (Figure 17) shows six exothermic peaks at 380 (broad), 510, 580, 850, 970, and 1015 C, and two endothermic peaks at 875 and 1070 C, respectively. The broad exothermic peak at 380 C may be due to oxidation of the organics. The exothermic peaks at 510, 580, and 850 C presumably represent crystallization of the lead germanate compounds. The DTA of PG 1(b) gel (Figure 18) shows an exothermic peak at 490 C absent in PG 1(a) gel. The DTA of basic lead acetate (Figure 23) shows that PbO crystallizes at approximately 500 C. Thus, it is apparent that crystallization of PbO took place in PG 1(b) gel, but no such crystallization was evident in PG 1(a) gel. Moreover, PG 1(a) gel shows an exothermic peak at 850 C absent in PG 1(b) gel. In PG 1(a) gel, the endothermic peak at 875 C is followed by two exothermic peaks at 970 and 1015 C. The endothermic peak at 875 C and the exothermic peak at 970 C may represent incongruent melting of a lead germanate compound. Note also that PbO melts in this temperature region. Therefore, the occurrence of the above endothermic and exothermic peaks may be due to melting of both PbO and a lead germanate compound. The exothermic peak at 1015 C may be due to the phase transformation of GeO_2 from Quartz to Rutile form. The endothermic peak at 1070 C may be due to melting of GeO_2 .

The DTA of PG 1(c) gel (Figure 20) shows many exothermic peaks representing crystallization/phase transformation temperatures and two endothermic peaks. However, the DTA of supercritically dried PG 1(c) gel (Figure 19) shows only a few exothermic peaks and two endothermic peaks. These exothermic and endothermic peaks are also present in PG 1(c) gel dried at 70 C. Observe that the nature of initial crystallization (up to about 600 C) of both PG 1(b) (Figure 18) and PG 1(c) (Figure 20) are similar and that PG 1(b) gel does not show DTA peaks in the 600 to 700 C temperature region. It is, therefore, apparent that the peaks in the above temperature range (Figures 18 and 20) do not represent phase transformations of lead germanate compounds but are indicative of crystallization temperatures. Comparing Figures 18 and 20 we also see that up to about 850 C the crystallization behavior of lead germanate gels depend on the drying technique; above 850 C the crystallization behaviors

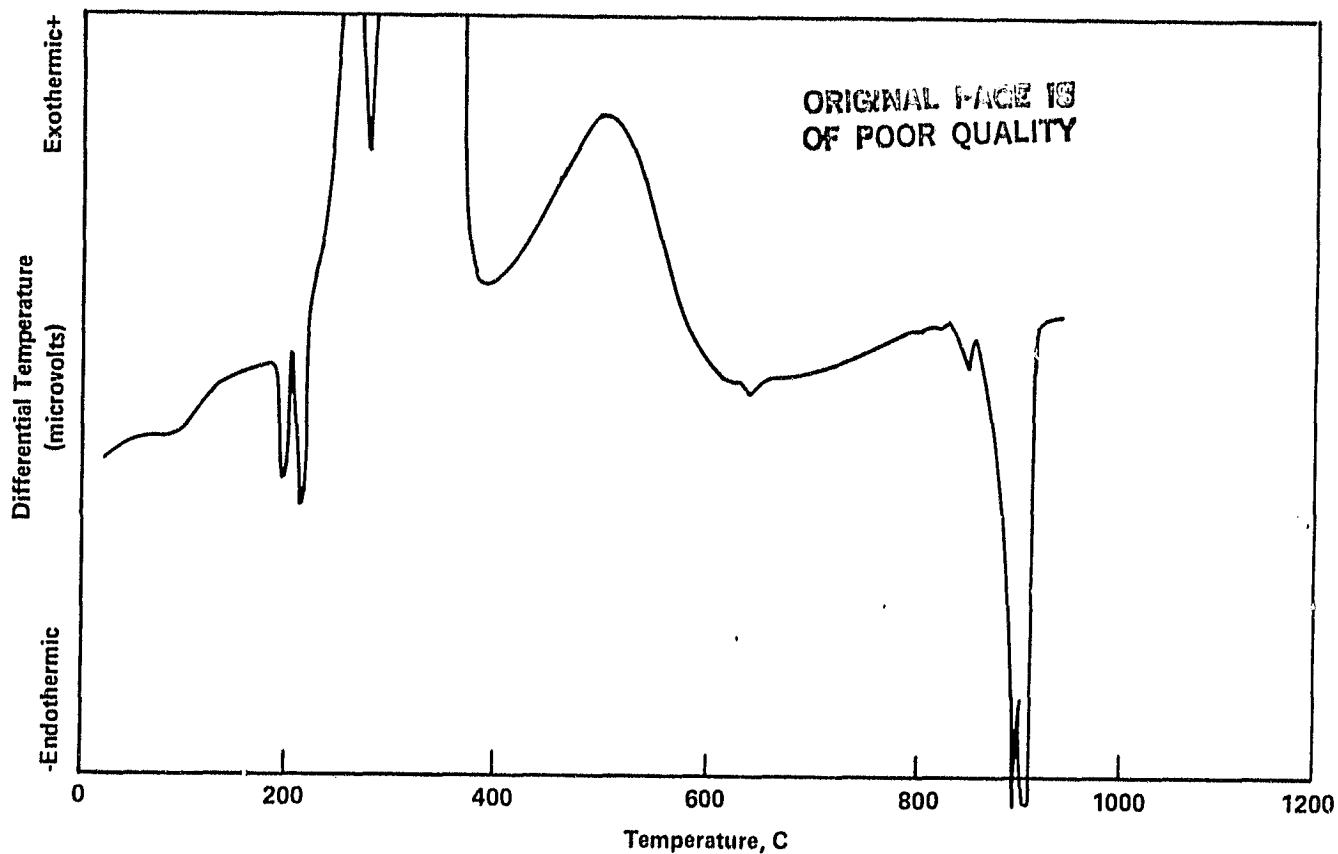


FIGURE 23. DIFFERENTIAL THERMAL ANALYSIS OF LEAD ACETATE (BASIC)

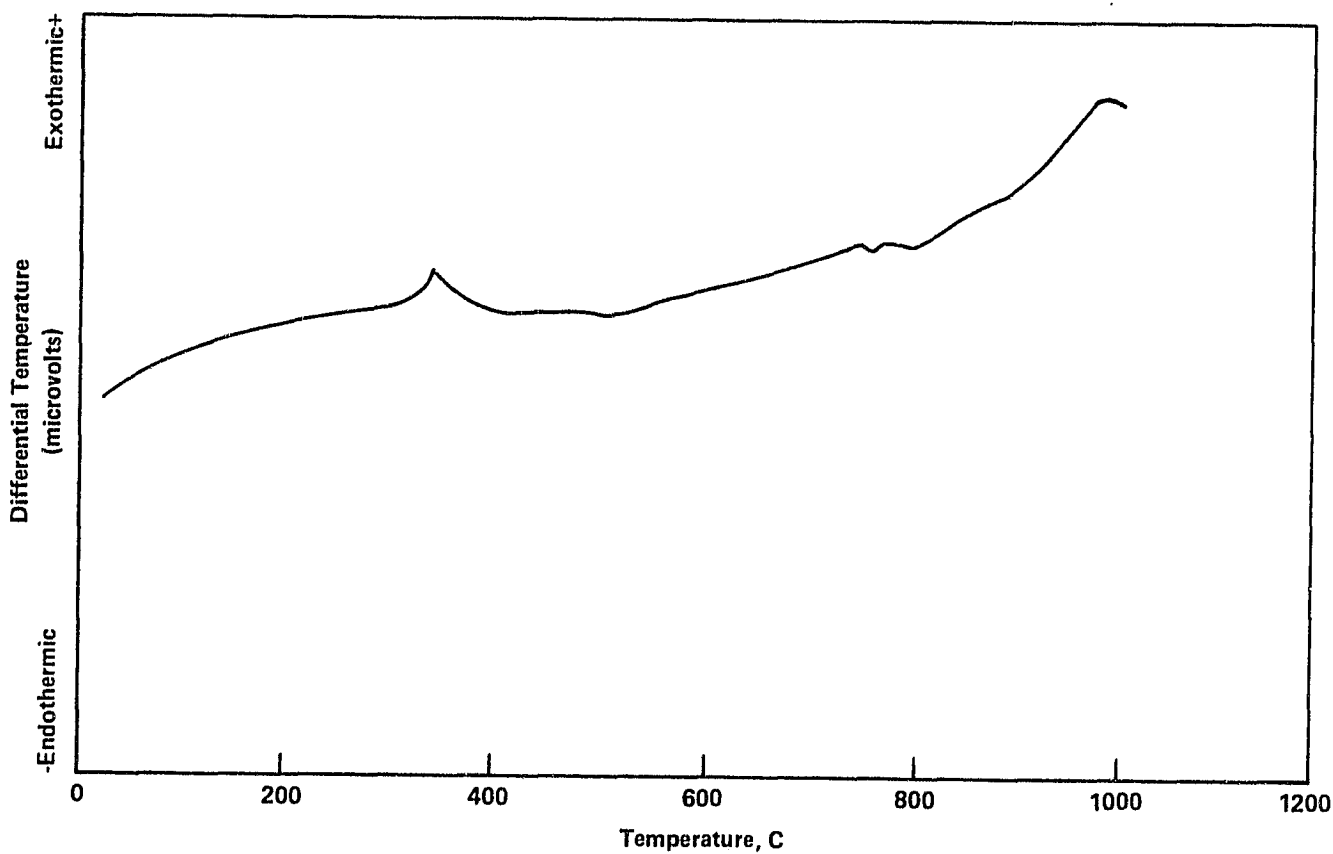


FIGURE 24. DIFFERENTIAL THERMAL ANALYSIS OF NONCRYSTALLINE GERMANIUM OXIDE

are similar. In both, a new crystalline phase appears between 860 and 870 C. The endothermic peak between 875 and 885 C, followed by an exothermic peak between 970 and 990 C, presumably represents incongruent melting behavior of a lead germanate compound. The endothermic peak at 1070/1090 C may be due to the melting of GeO_2 . The difference in peak sizes is evidently related to the relative amounts of GeO_2 .

The DTA curve of PG 2(b) gel (Figure 21) is qualitatively similar to PG 1(b) gel except that PG 2(b) gel shows one additional exothermic peak at 330 C and two additional endothermic peaks at 400 and 755 C. The exothermic peak at 330 C may be due to the thermal decomposition of lead acetate. However, the occurrence of the endothermic peak at 400 C could not be readily understood. (IR studies indicate that free lead acetate is present in the gel. See IR spectrum in Figure 10.) Presumably, the presence of free lead acetate in the PG 2(b) gel resulted in the formation of a low temperature eutectic composition represented by the endothermic peak at 755 C. The DTA curve of PG 3(b) gel (Figure 22) shows two very small crystallization peaks at 465 and 515 C. The two exothermic peaks presumably correspond to the peaks at 530 and 575 C of the PG 2(b) gel (Figure 21). The shift in the peak temperature (60-65 C in each case) may be related both to amounts of the crystalline phases and the probable differences in the actual heating rate. Observe that the endothermic peak of the PG 3(b) gel at 750 C is smaller than the endothermic peak of PG 2(b) gel at 755 C, even though the amount of free lead acetate in PG 3(b) gel is more than in PG 2(b) gel. The reason for the relatively smaller endothermic peak with the PG 3(b) gel may be related to the amount of free GeO_2 available. Presumably, the presence of increasing amounts of free lead acetate decreases the availability of free GeO_2 . The endothermic peaks at 815 C (PG 2(b) gel) and 805 C (PG 3(b) gel) may represent melting of the same lead germanate compound or the same eutectic composition; and the differences in the peak sizes may be related to their relative amounts.

Differential thermal analyses indicate that the crystallization behavior of the lead germanate gels depend on:

- gel composition
- gel preparation procedure
- initial drying procedure
- presence of free lead compound in the as-prepared gel.

X-ray Diffraction Analysis--X-ray diffraction analyses were performed on all the samples listed in Table 9. The d-values obtained with the test samples are listed in Tables 11 and 12; the d-values of the crystalline phases of lead germanate compounds (as reported in the literature), are listed in Table 13. Except the as-prepared PG 1(c) gel, all X-ray diffraction studies were performed by the powder method. PG 1(a) and PG 1(b) gels after drying at 70 C were noncrystalline. As-prepared PG 1(c) gel in the paste form was packed in a sample holder consisting of a glass backing and a ring, 25 mm inner diameter and 1 mm thick. The sample was dried in a vacuum desiccator. The diffraction pattern showed a broad band with a maximum at 26.25 degrees (2θ). Subsequently, the gel was air dried, reduced to powder by gentle grinding, packed into a piece of double-sided scotch tape for mounting in the diffractometer. Then an X-ray run was taken. This time the broad band was somewhat sharper with a maximum of 26.5 degrees 2θ ($d = 3.357\text{\AA}$); and an extremely weak band appeared at approximately 38.6 degrees (2θ) ($d = 2.332\text{\AA}$). The position of the above bands corresponds closely to the crystalline peaks of hexagonal germanium oxide ($d = 3.429$ and 2.366\AA). The following conclusions, therefore, can be drawn from the X-ray diffraction results of the as-prepared PG 1(c) gel.

- As-prepared gel was noncrystalline.
- The gel showed tendency to crystallize during drying under ambient condition.
- Hexagonal GeO_2 tended to appear as the crystalline phase during drying.

The diffraction pattern of PG 1(c) gel dried at 70 C was very similar to that of crystalline germanium oxide (hexagonal). Also, this sample showed two broad bands ($d = \sim 3.45$ and $\sim 2.71\text{\AA}$) and two peaks at $d = 2.002\text{\AA}$ (relatively large) and $d = 1.483\text{\AA}$ (very small). The positions of these bands/peaks may indicate that either PbGeO_3 or PbGe_2O_5 , or both these lead germanate compounds, tended to appear during drying at 70 C. PG 1(b) gel after thermal treatments to 500 and 600 C apparently indicated the presence of three crystalline phases in both cases, namely, PbGe_4O_9 , PbGeO_3 , and GeO_2 (hexagonal). Moreover, the gel thermally treated to 600 C shows an additional peak with d value 3.108\AA which might be due to crystallization of PbO . However, this could not be confirmed.

TABLE 11. d SPACINGS OF PG 1(a) AND PG 1(c) GELS AFTER DIFFERENT THERMAL TREATMENTS

	PG 1(b) Gel			As-Prepared Wet	PG 1(c) Gel	
	Dried at 70 C	500 C	600 C		1000 C	Dried at 70 C
						7.124 (4)
	6.31 (3)					6.29 (5)
N	5.731 (9)	5.717 (10)				
O			5.619 (5)			
N						5.55 (8)
C	4.695 (2)					4.733 (6)
R		4.630 (2)				4.642 (6)
Y		4.516 (2.5)				
S	4.311 (16)	4.312 (11)				
T			4.256 (7)		4.25 (19)	4.295 (19)
A	4.202 (10)	4.197 (12)				
L			4.137 (8)			
L	3.798 (5)	3.794 (3.5)				3.740 (23)
I	3.658 (42)	3.657 (35)				
N						3.566 (47)
E						3.474 (7)
	3.433 (~150)	3.434 (~100)			3.45 B	3.417 (100)
			3.387 (36)	3.375 B	3.391 (100)	3.323 (57)
	3.302 (7)	3.290 (10)	3.356 (6)			
			3.274 (6)			3.212 (9)
		3.108 (13)	3.077 (100)			3.108 (10)
			2.975 (2)			2.964 (32)
	2.929 (26)	2.917 (33)	2.889 (23)			
	2.860 (30)	2.853 (29-1/2)	2.840 (13)			2.844 (12)
						2.833 (9)
						2.780 (18)
						2.729 (24)
	2.709 (29)	2.702 (24)			2.71 B	
						2.682 (24)
			2.627 (3)			2.663 (20)
						2.553 (4)
	2.496 (10)	2.491 (4-1/2)	2.468 (3)			
		2.394 (6-1/2)	2.380 (100)		2.471 (8)	2.480 (15)
	2.368 (26)	2.360 (20)	2.346 (7)		2.345 (15)	2.354 (19)
	2.282 (14)	2.279 (8)		2.332 B		2.330 (18)
		2.255 (3-1/2)	2.259 (5)		2.262 (10)	2.276 (10)
	2.191 (8)	2.192 (9-1/2)	2.186 (38)		2.143 (15)	2.152 (18)
	2.163 (22)	2.163 (16)	2.154 (3)		2.002 (19)	1.970 (8)
	2.103 (3)		2.145 (4)			
	2.046 (3.5)	2.044 (3-1/2)	2.093 (20)			1.913 (8)

ORIGINAL PAGE IS
OF POOR QUALITY

TABLE 11. (Continued)

ORIGINAL PAGE IS
OF POOR QUALITY

Dried at 70 C	PG 1(b) Gel			As-Prepared Wet	PG 1(c) Gel	
	500 C	600 C	1000 C		Dried at 70 C	Supercritically Dried
2.001 (4)						
1.965 (9)		1.961 (8)	1.955 (7)		1.872 (2)	1.874 (9)
1.870 (12)		1.870 (7)	1.858 (4)		1.857 (8)	1.865 (9)
1.827 (10)		1.823 (8-1/2)	1.816 (4)			1.823 (19)
						1.8072 (4)
1.770 (10)		1.770 (8)	1.765 (4)			1.789 (10)
		1.745 (2-1/2)				1.748 (4)
1.716 (5)		1.715 (4)			1.719 (2)	1.725 (6)
					1.708 (5)	
1.663 (2)		1.658 (5)	1.651 (3)			1.664 (7)
1.648 (7)		1.649 (6)				1.544 (7)
1.630 (4)		1.622 (3-1/2)			1.622 (2)	
			1.614 (96)			1.583 (1)
1.569 (14)		1.567 (8)	1.560 (5)		1.560 (9)	1.565 (7)
			1.548 (18)			
		1.538 (3)	1.533 (4)			1.534 (2)
						1.510 (1)
1.503 (7)		1.500 (4)			1.496 (2)	1.497 (5)
		1.491 (2-1/2)			1.483 (2)	1.481 (3)
1.458 (3.5)		1.456 (4)				1.453 (4)
			1.428 (4)		1.413	
1.415 (20)		1.414 (11)	1.414 (3)		1.407 (8)	1.402 (10)
			1.410 (5)			
1.397 (10)		1.396 (7-1/2)			1.389 (5)	1.393 (5)
			1.387 (13)			
1.370 (3)						1.370 (2)
1.356 (5)					1.337 (3)1	1.343 (4)
1.340 (7)		1.340 (3)	1.301 (16)			
1.282 (5)		N	1.297 (15)		1.278 (3)	
		O				1.265 (2)
		T				1.249 (2)
1.228 (3.5)						1.230 (2)
1.199 (6)		M	1.197 (6)			1.193 (4)
		E				1.169 (3)
		A	1.152 (3)			
		S				1.143 (2)
		U				
		R	1.120 (7)			
1.1023 (2)		E	1.098 (10)			
1.068 (3)		D				

ORIGINAL PAGE 13
OF POOR QUALITY

TABLE 12. d SPACINGS OF PG 2(b) AND PG 3(b) GELS

PG 1(a) Gel (Dried at 70 C)	PG 2(b) Gel (Dried at 70 C)	PG 3(b) Gel (Dried at 70 C)
Noncrystalline	4.64 (4) Small band 3.52 (14) Broad band 2.74 (10) Very broad band 2.316 (4) Broad band 2.149 (3) Broad band 1.868 (2) Broad band 1.789 (3) Broad band	~5.62 (2) Small band ~4.56 (2) Small band ~3.92 (3) Small band 3.705 (4) Somewhat sharp peak 3.456 (8) Somewhat sharp peak 3.108 (2) Small band 2.895 (4) Small band 2.316 (3) Small band

TABLE 13. d SPACINGS OF COMPOUNDS IN THE GeO₂-PbO SYSTEM
(REF: J. AM. CERAM. SOC 48 (8), 1965, 400)

Pb ₄ GeO ₆		Pb ₃ Ge ₂ O ₇		Pb ₆ GeO ₃		Pb ₆ Ge ₂ O ₅		Pb ₆ Ge ₄ O ₉	
d Spacing (Å)	Relative Intensity	d Spacing (Å)	Relative Intensity	d Spacing (Å)	Relative Intensity	d Spacing (Å)	Relative Intensity	d Spacing (Å)	Relative Intensity
7.500	10	7.462	30	6.559	10	7.081	20	5.754	15
3.278	10	3.708	25	5.945	25	4.095	25	4.230	20
3.175	85	3.363	70	4.396	10	3.883	20	3.678	70
3.121	65	3.314	35	3.633	50	3.754	20	3.414	5
3.069	100	3.209	55	3.427	100	3.648	65	3.314	35
2.950	20	2.959	100	3.326	40	3.548	40	2.931	60
2.894	10	2.931	95	3.164	25	3.440	30	2.867	100
2.771	60	2.849	60	3.121	55	3.351	25	2.714	80
2.683	10	2.080	80	3.048	40	3.243	70	2.380	30
2.637	10	2.027	45	2.988	45	3.132	90	2.315	5
2.508	10	2.002	35	2.940	20	3.058	5	2.196	30
2.430	5	1.937	40	2.885	60	2.998	5	2.166	25
2.338	5	1.903	45	2.797	60	2.950	90	2.108	5
1.933	15	1.884	70	2.739	50	2.885	30	2.053	20
1.884	20	1.804	40	2.667	25	2.763	30	1.969	50
1.855	35	1.781	25	2.600	30	2.722	100	1.933	20
1.845	30	1.701	25	2.522	10	2.514	20	1.907	5
1.698	10	1.656	25	2.411	25	2.362	50	1.828	55
1.681	10	1.593	30	2.362	60	2.141	60	1.797	15
1.647	10	1.573	25	2.265	10	2.103	30	1.768	40

TABLE 13. (Continued)

Pb ₄ Ge ₆		Pb ₃ Ge ₂ O ₇		PbGeO ₃		PbGe ₂ O ₅		PbGe ₄ O ₉	
d Spacing (Å)	Relative Intensity	d Spacing (Å)	Relative Intensity	d Spacing (Å)	Relative Intensity	d Spacing (Å)	Relative Intensity	d Spacing (Å)	Relative Intensity
1.616	10	1.5		2.233	15	2.019	55	1.650	50
1.590	20			2.191	15	1.949	20	1.595	10
				2.094	30	1.746	40		
				2.076	35	1.707	20		
				2.006	10	1.664	20		
				1.985	25	1.647	20		
				1.945	10	1.610	20		
				1.899	10	1.578	20		
				1.873	10	1.556	20		
				1.848	15				
				1.807	20				
				1.791	30				
				1.781	30				
				1.737	45				
				1.689	10				
				1.664	20				
				1.653	20				
				1.608	35				
				1.588	35				
				1.563	10				

ORIGINAL PAGE IS
OF POOR QUALITY

The diffraction pattern of supercritically dried PG 1(c) gel shows a large number of diffraction peaks. A proper and accurate analysis of this result proved very difficult because of the presence of many crystalline phases having similar diffraction patterns. However, the results indicate that the supercritically dried PG 1(c) may be constituted of a complex mixture of GeO_2 , PbO , PbGeO_3 , PbGe_2O_5 , and PbGe_4O_9 . The diffraction pattern of PG 1(b) after thermal treatment up to 1000 C (Sl No. 5, Table 9) shows the presence of GeO_2 , PbGe_4O_9 , PbO , and perhaps PbGeO_3 .

PG 2(b) gel after drying at 70 C showed a number of broad bands which indicate that the gel was partially crystalline. The bands with maxima at approximately $d = 4.64, 3.52, 2.316, 2.159, \text{ and } 1.870\text{\AA}$ (Table 12) correspond closely to the strongest diffraction peaks of crystalline germanium oxide (hexagonal). However, the bands with maxima at approximately 2.74 and 1.789 could not be readily identified.

PG 3(b) gel after drying at 70 C was also found to be partially crystalline. A somewhat sharp peak at $d = 3.456\text{\AA}$ and two small bands at $d = 4.56$ and 2.316\AA in the diffraction pattern of this gel indicate the presence of partially crystalline germanium oxide. A somewhat sharp (though small) peak at $d = 3.705\text{\AA}$ and the band maxima at $d = 5.62, 3.108, \text{ and } 2.895\text{\AA}$ correspond closely to the characteristic diffraction pattern of lead (II) acetate, $(\text{CH}_3\text{COO})_2\text{Pb}$. The IR spectrum of this gel (Figure 11) indicates the presence of free lead acetate, appearing to confirm the X-ray results.

The following conclusions can be drawn from the X-ray studies:

- Crystallinity of the as-prepared gel depends on the preparation procedure.
- Crystallinity of the dried gel depends on the drying procedure.
- Noncrystalline gel on thermal treatment decomposes into many crystalline compounds.
- The presence of many crystalline phases and the similarity between the diffraction patterns of lead germanate compounds make it difficult to identify accurately the crystalline phases.

Conversion of Gels to Glasses

Two different techniques were adopted for converting gels to glasses:

- Sintering of gel monoliths
- Melting of gel powders.

Glasses were also prepared by melting conventional glass batches.

SiO₂-GeO₂ System. A supercritically dried gel monolith, SG 2(b), was sintered in an oxygen atmosphere at 1280 C. The heating schedule as shown in Figure 25 was based on the sintering behavior of the gel monolith observed by thermal dilatometric analysis. The thermal dilatometric analysis curve of the gel monolith is shown in Figure 26. It is evident from the curve that the sintering starts at a slower rate from 400 C, but sintering at an enhanced rate occurs from 1000 C and completes at 1200 C. It is evident from the curve that sintering starts at a slow rate from 400 C but at an enhanced rate from 1000 C and completes at 1200 C.

GeO₂-PbO System. Lead germanate gel monoliths completely lost their integrity on supercritical drying, thus the sintering of gel monoliths to glass was not feasible. Therefore, gel-derived lead germanate glasses were prepared by melting the gel powders. Lead germanate glasses of the following compositions were prepared.

<u>Composition (Mol Percent)</u>	<u>Preparation Route</u>
10 Pb0.90 GeO ₂	Gel-derived (from air-dried gel)
10 Pb0.90 GeO ₂	Gel-derived (from supercritically dried gel)
10 Pb0.90 GeO ₂	Conventional
33 Pb0.67 GeO ₂	Conventional
50 Pb0.50 GeO ₂	Conventional

ORIGINAL PAGE 19
OF POOR QUALITY

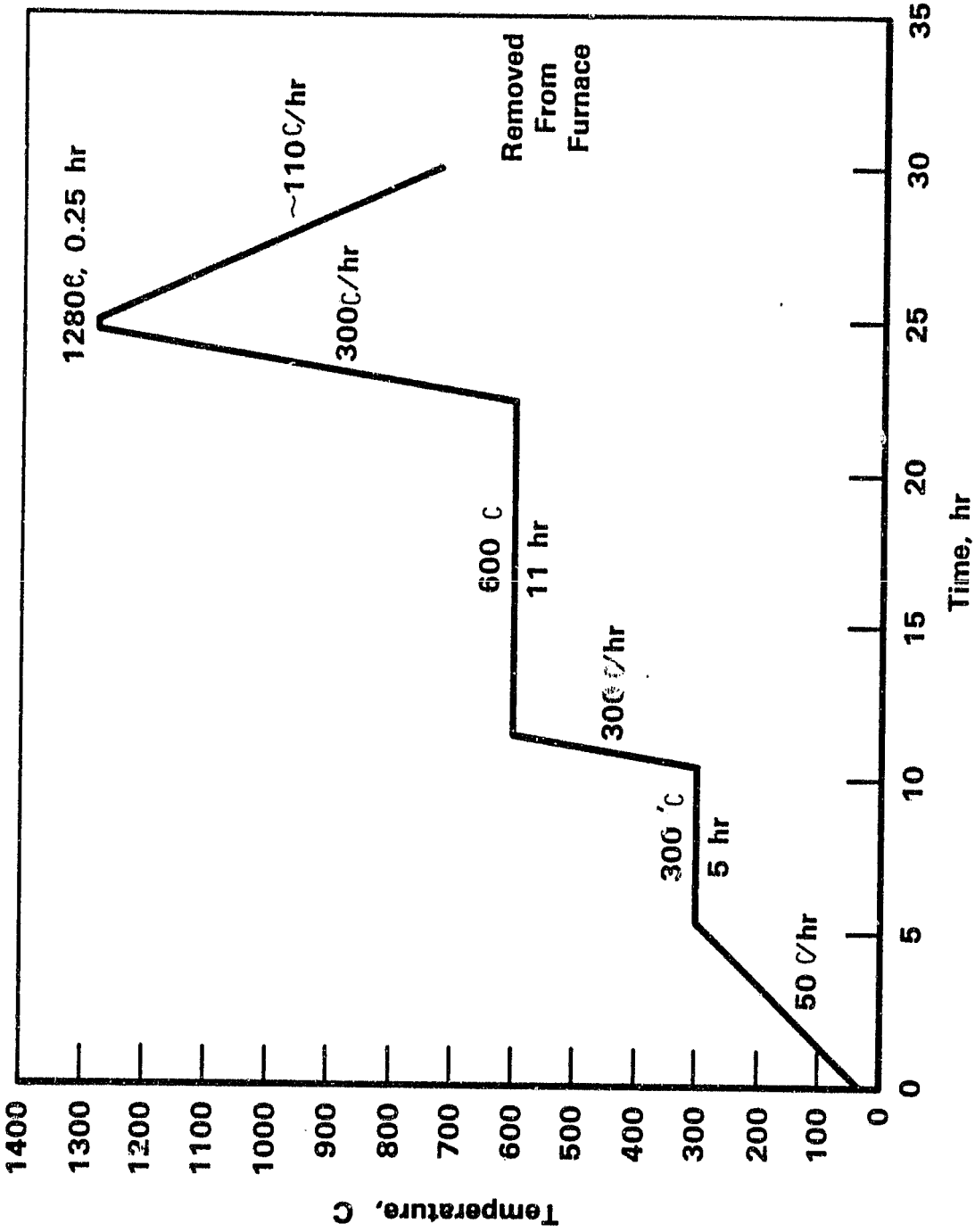


FIGURE 25. HEATING SCHEDULE FOR THE SINTERING OF GEL MONOLITH OF COMPOSITION SG 2

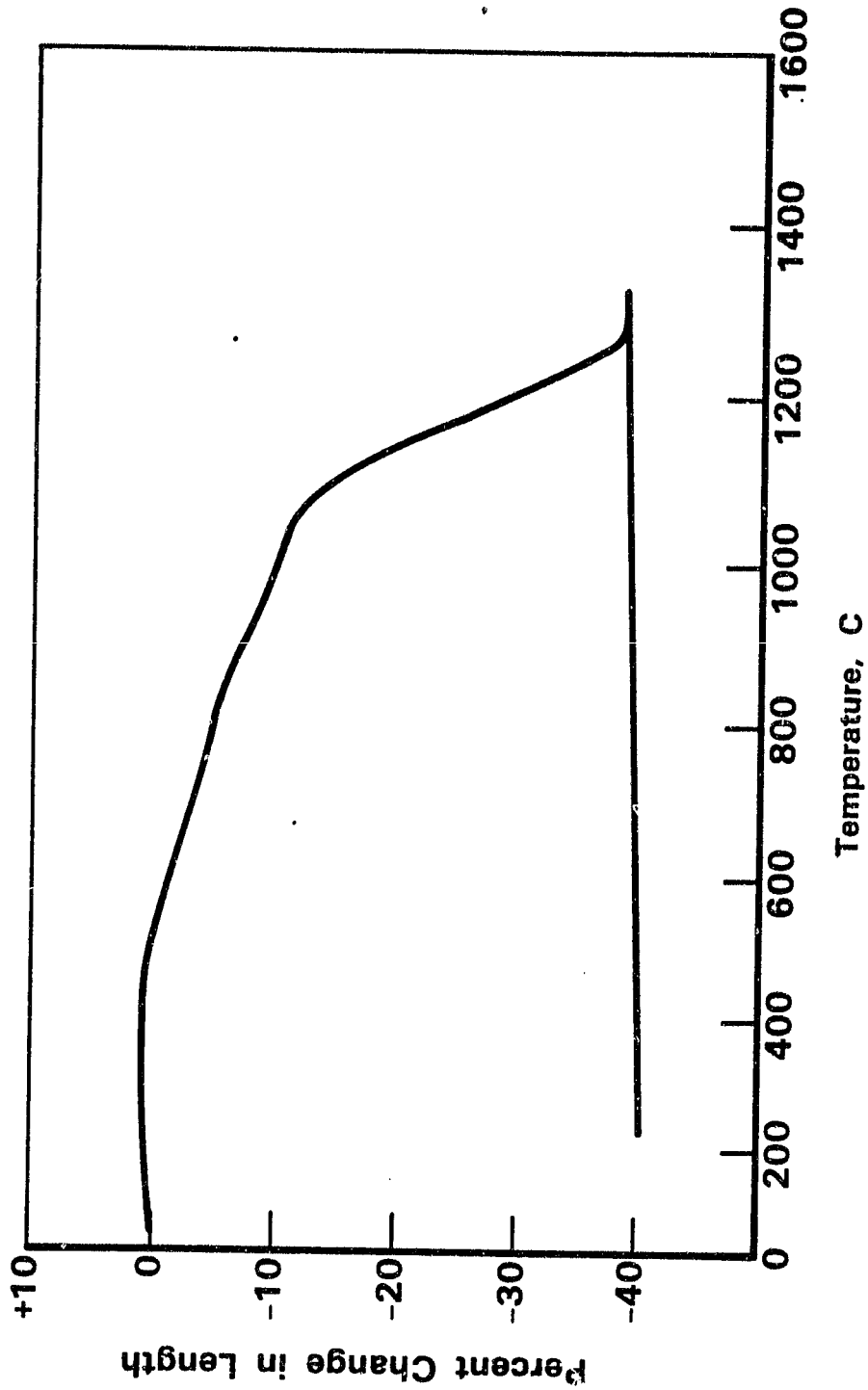


FIGURE 26. THERMAL DIALATOMETRIC CURVE OF A GEL MONOLITH OF COMPOSITION SG 2

Preparation of Gel-Derived Glasses. Gel powders dried at 70 C were placed in a platinum crucible which was directly introduced into a furnace at 1000 C under ambient air atmosphere. The temperature of the furnace, raised to the desired melting temperature, was held at that temperature for a specified time. The crucible was then taken out of the furnace and quenched in air. The crucible containing the glass was annealed by heating at the rate of 20 C/hr and holding at the annealing temperature for two hours.

Preparation of Glasses by Melting Conventional Batch Material.

Ultrapure germanium dioxide (GeO_2) and reagent grade lead oxide, PbO (99.9 percent pure, -60 mesh), were mixed under anhydrous alcohol, dried under infrared lamp, and then melted in a platinum crucible in an electric furnace under ambient atmosphere. The platinum crucible containing the mixed oxides was introduced into the furnace at about 1000 C. The furnace temperature was raised to the desired level and held at that temperature for a specified time. Clear and apparently bubble-free glass was poured in a mold, and quenched in air. The glasses were annealed by heating at the rate of 20 C/hr and holding at the annealing temperature for two hours. The melting and annealing temperatures for the lead germanate glasses are shown in Table 14.

Characterization of Glasses in the GeO_2 - PbO System. The gel-derived and the conventionally prepared 10 PbO .90 GeO_2 composition glasses were characterized as follows:

- Chemical composition by X-ray fluorescence spectroscopy
- Molecular structure by infrared spectroscopy
- Crystallization behavior by differential thermal analysis.

Chemical Analyses--Both gel-derived and conventionally prepared PG-1 glass samples were chemically analyzed to examine compositional changes occurring during melting. The glass samples were fused with lithium tetraborate and analyzed by X-ray fluorescence spectroscopy. The results are shown in Table 15. The starting batch composition (weight percent) of the above glasses was PbO :19.2, GeO_2 :80.8.

The results indicated about one percent loss of PbO during preparation of the conventional glass (due to evaporation of PbO during melting).

TABLE 14. MELTING AND ANNEALING TEMPERATURES OF LEAD GERMANATE GLASSES

Composition (Mol Percent)	Preparation Route	Melting Parameters			Annealing Temperature (C)
		Temperature (C)	Holding Time (Hr)	Atmosphere	
10 Pb0.90 GeO ₂	Gel dried at 70 C	1200	1	Ambient	440
10 Pb0.90 GeO ₂	Gel dried at 70 C	1200	3	Ambient	440
10 Pb0.90 GeO ₂	Supercritically dried gel	1200	3	Ambient	440
10 Pb0.90 GeO ₂	Conventional (single melting)	1200	3	Ambient	440
10 Pb0.90 GeO ₂	Conventional (double melting)	1200	3	Ambient	440
33 Pb0.67 GeO ₂	Conventional		3	Ambient	410
50 Pb0.50 GeO ₂	Conventional		3	Ambient	350

TABLE 15. CHEMICAL COMPOSITIONS OF PG 1 GLASSES

Sample	Composition (Weight Percent)	
	PbO	GeO ₂
Gel-derived glass	19.7±0.2	80.1±0.2
Conventional glass	18.1±0.2	81.0±0.2

However, the gel-derived glass showed an increase of 0.5 percent PbO from the starting composition. This increase in PbO in the gel-derived glass was attributed to the molecular composition and the purity of the starting compounds. To check the validity of the above assumptions, germanium ethoxide and basic lead acetate used for the preparation of the lead germanate gels were analyzed for their metal content. The results of the chemical analyses and the calculated values based on the molecular formulae are shown below.

Sample	Analyte	Concentrations (Weight Percent)	
		As Analyzed	As Calculated From Molecular Formula
Lead Basic Acetate (CH ₃ COO) ₂ Pb·Pb(OH) ₂	Pb	73.9	73.151
Ge(OC ₂ H ₅) ₄	Ge	28.0	28.709

Based on the results of chemical analyses the actual starting composition of PG-1 gel calculated to 100 percent was as follows:

PbO:19.75, GeO₂:80.25.

The results of the chemical analysis of the gel-derived glass calculated to 100 percent was as follows:

PbO:19.74, GeO₂:80.26.

The above results indicate that there was practically no loss of lead (PbO) during preparation of the gel-derived lead germanate glass (Composition PG-1). Therefore, it can be concluded that the sol gel route was effective in controlling the lead germanate glass composition under study.

Molecular Structure--The molecular structures of both gel-derived and conventional PG-1 glasses were examined by infrared spectroscopy. The infrared spectra of the gel-derived and the conventional glasses are shown in Figures 27 and 28 respectively. It appears that in both glasses the dominant absorption due to Ge-O-Ge stretching are at about 11.8 μm ($\sim 850\text{ cm}^{-1}$ wave-number) indicating that the coordination characteristics of GeO₂ and PbO are similar in both the glasses.

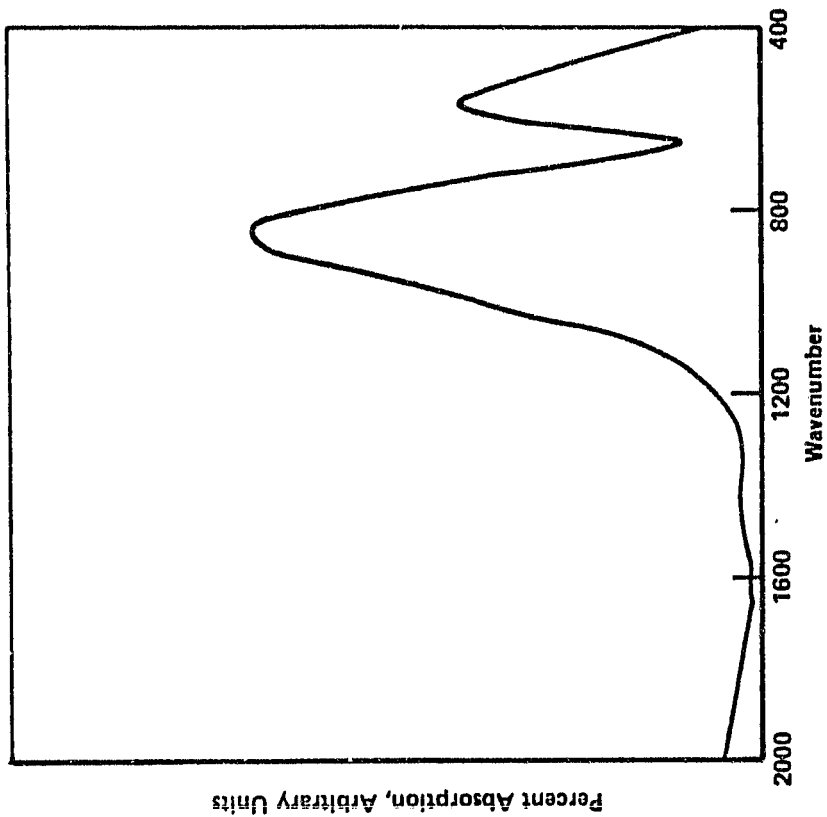


FIGURE 28. INFRARED SPECTRUM OF CONVENTIONALLY
MELTED PG 1 GLASS, 1200 C/5 HR

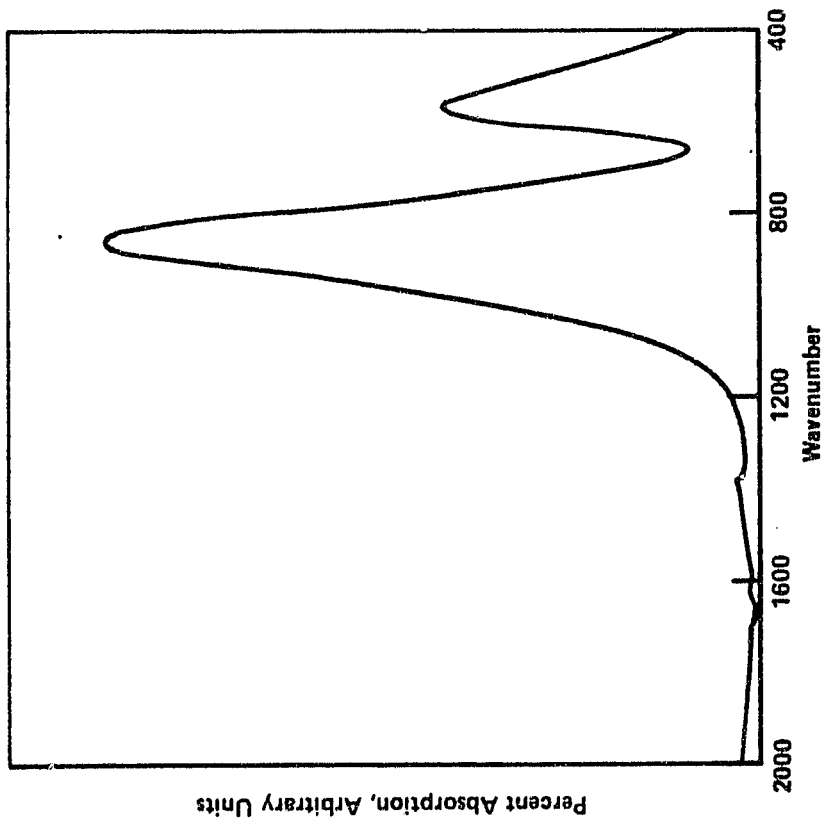


FIGURE 27. INFRARED SPECTRUM OF GEL-DERIVED
PG 1 GLASS, 1200 C/3 HR

Differential Thermal Analysis--The differential thermal analyses of lead germanate glasses were performed in static air up to 1000 C at the heating rate of 10 C/min. The DTA curves are shown in Figures 29 and 30. The nature and position of the DTA peaks are listed in Table 16.

TABLE 16. DTA OF GEL-DERIVED AND CONVENTIONAL LEAD GERMANATE GLASS

Gel-Derived PG 1 Glass		Conventional PG 1 Glass	
Temperature (C)	Nature of Peak	Temperature (C)	Nature of Peak
		460	Exo
490	Endo	--	--
580	Exo	580	Exo
615	Exo	620	Exo
690	Exo (Extremely small)	--	--
825	Endo	820	Endo
840	Endo	840	Endo

Observe that the DTA curve of the conventional glass shows an exothermic peak at about 460 C absent in the DTA curve of the gel-derived glass. We have assumed that this exothermic peak represents crystallization of PbO from the region of the glass rich in PbO. This assumption is based on the fact that the DTA of basic lead acetate shows an exothermic peak at the same temperature (Figure 23). Therefore, the occurrence of the exothermic peak at 460 C may be related to nonhomogeneity of the conventional glass. The gel-derived glass shows an endothermic peak at 490 C absent in the DTA curve of the conventional glass. The endothermic peak may represent the glass transition temperature. The absence of the endotherm in the DTA curve of the

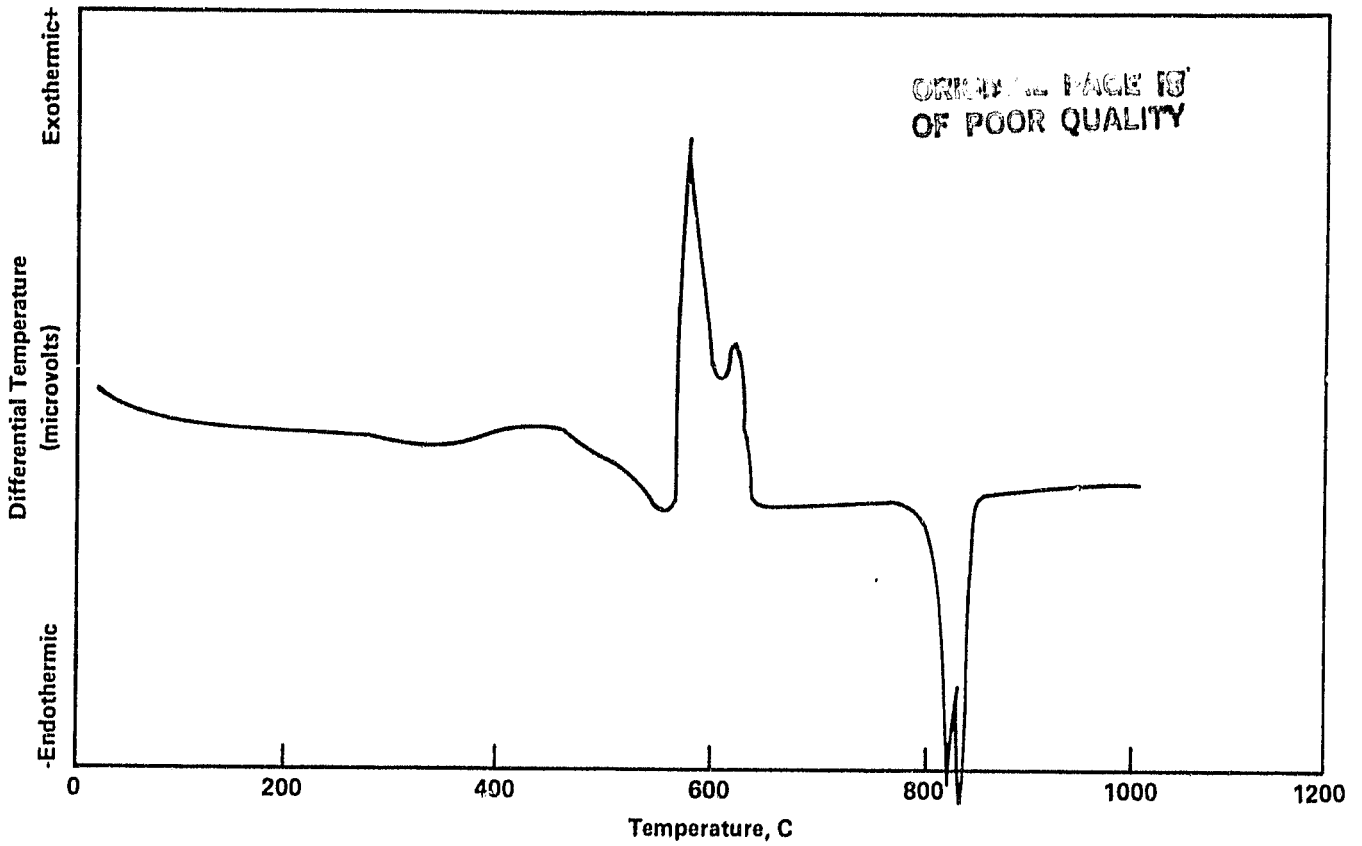


FIGURE 29. DIFFERENTIAL THERMAL ANALYSIS OF CONVENTIONAL PG 1 GLASS

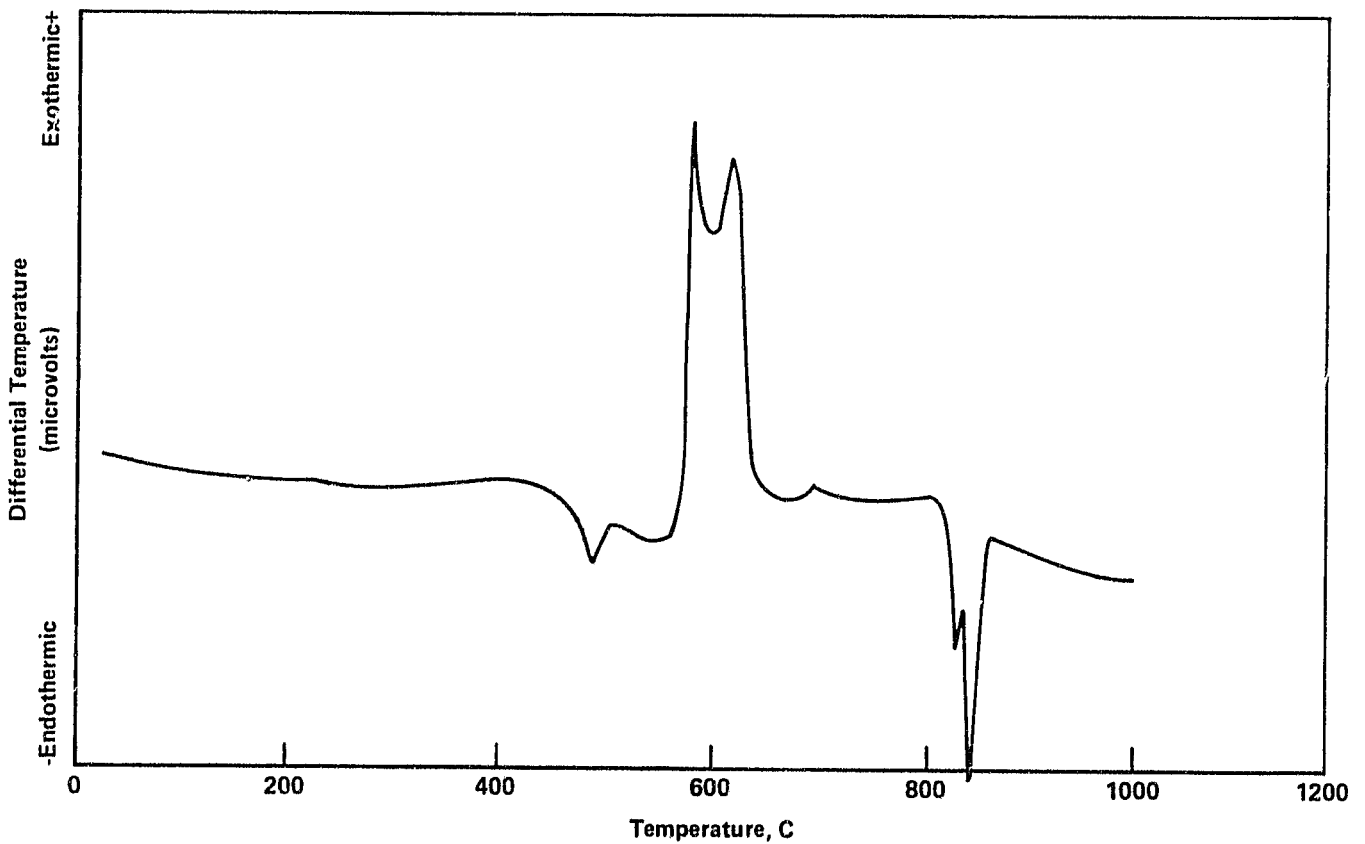


FIGURE 30. DIFFERENTIAL THERMAL ANALYSIS OF GEL-DERIVED PG 1 GLASS

conventional glass may be due to the fact that the endotherm (because of glass transition) was masked in the exothermic peak around the same temperature. Both glasses show exothermic peaks at 580 and ~ 620 C. However, the relative amounts of crystalline phases determined by the areas under the peaks were different. It is, therefore, obvious that the crystallization behaviors of the gel-derived and conventionally prepared glasses were different. Further, both the glasses show endothermic peaks at about 820 and 840 C. Presumably, these endothermic peaks represent melting of the crystalline phases, not eutectics. This assumption is based on the observed correlations between the areas of the endothermic and the exothermic peaks. Probably the crystalline phase with the exothermic peak at 580 C melts at about 820 C, and the crystalline phase with the exothermic peak at about 620 C melts at 840 C. Note also that for conventional glass the above correlation does not appear to apply strictly. This may be because lead oxide forming in the conventional glass also melted in this temperature region.

The following conclusions can be drawn from the DTA results on the PG-1 glasses.

- Crystallization behaviors of the gel-derived and the conventional glasses are different.
- Crystallization behavior is related to glass homogeneity.

Thermal Treatment of Levitated Gel Monolith. Composition SG 2 porous gel monolith was thermally treated in an acoustic levitator located at Interasonics, Inc. The details of the experimental procedures and the results obtained from Interasonics, Inc., are reproduced below:

On March 14, 1983, a test specimen was processed in the pressure facility at Interasonics, Incorporated. The specimen was supplied by Dr. Mukherjee, who attended the test. It consisted of a gel solid of 90 percent SiO₂ and 10 percent GeO₂, about 5 mm in diameter, but of irregular shape. The processing pressure was 75 psig at the start and increased to 85 at the end. The specimen was levitated successfully with reasonable stability at various furnace temperatures during heat-up, and finally it was suspended without contact for about 20 minutes, as the temperature rose from 875 C to 1225 C.

The Hot Zone temperature curve was obtained from data extracted from the videotape. The first 15 minutes of the run were omitted from the graph as there was no levitation during that period. The temperature rise during that period was approximately 20 C/min.

It did not appear that the specimen underwent much densification and therefore a second run was made on March 16 to obtain a temperature calibration of the specimen. A platinum-rhodium thermocouple was embedded in a specimen of the same approximate size and held stationary in the energy well. On this run the temperature profile was held as close as possible to that of the first run as measured by the Hot Zone thermocouple. It is clear from the plot that the sound created large temperature shifts, with time constants of approximately 5 sec. Our final equilibrium temperature of the specimen was approximately 950 C, well below the melting point of that particular specimen. At the end of the duplicate run, the specimen was allowed to densify by turning off the sound. The specimen temperature reached 1300 C very rapidly and it was allowed to soak for about 1 minute. After cooling, examination of the specimen showed a white, crystallized specimen with a density of 2 gm/cm³. Additionally there did not appear to be any noticeable bubbling or foaming during the melting process.

The curve showing Hot Zone vs specimen temperature in a test run is shown in Figure 31.

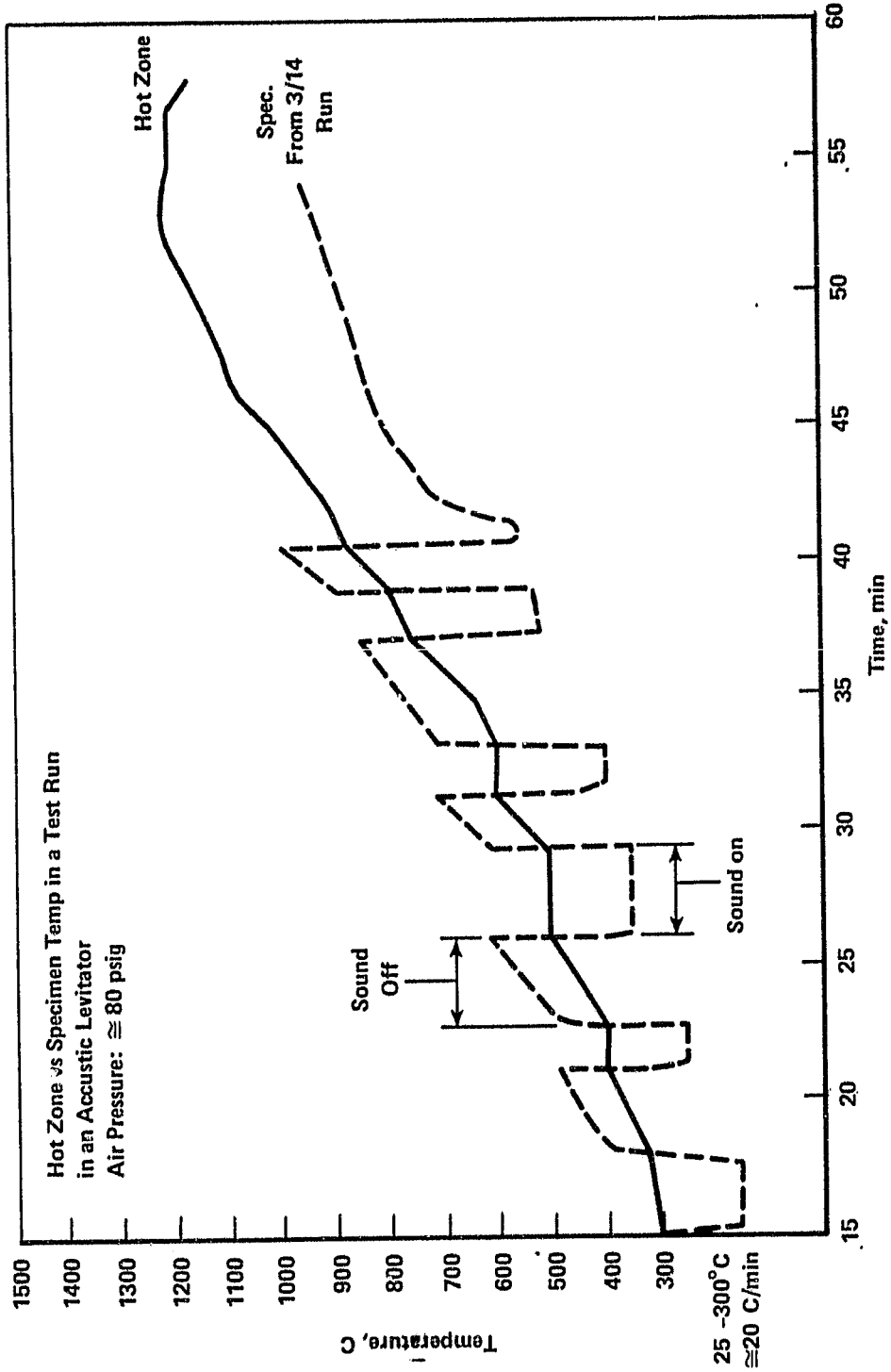


FIGURE 31. HOT ZONE VS SPECIMEN TEMPERATURES DURING LEVITATED SINTERING

CONCLUSIONS

The following conclusions can be drawn from the results of the present investigations.

SiO₂-GeO₂ System

- Noncrystalline gels and gel monoliths can be prepared with all the compositions studied.
- Gel monoliths can be supercritically dried without any loss of integrity.
- Composition 95 SiO₂ · 5GeO₂ gel does not show crystallization tendency on thermal treatment up to 1300 C. However, Compositions 90 SiO₂ · 10 GeO₂, 44 SiO₂ · 56 GeO₂, and 20 SiO₂ · 8 GeO₂ showed crystallization tendency on thermal treatment at higher temperatures (800-1200 C).
- Composition 90 SiO₂ · 10 GeO₂ gel monolith can be completely densified by thermal treatment at approximately 1280 C.
- Composition 90 SiO₂ · 10 GeO₂ gel monoliths can be levitated in an acoustic levitator during thermal treatment up to 900 C.

GeO₂-PbO System

- Noncrystalline lead germanate gels and gel monoliths can be prepared by the sol gel process.
- The gel monoliths lose integrity upon supercritical drying due to breakdown of the gel structure.
- Lead germanate gels crystallize on thermal treatment in different crystalline phases. The nature of the crystalline phases depends on the composition, the gel preparation procedure, and the drying technique.
- Glasses can be prepared from lead germanate gels by melting.
- Lead germanate glass composition can be effectively controlled by following the sol gel route.

- The crystallization behaviors of gel-derived and conventional lead germanate glasses are different.

SiO₂-TiO₂ System

- Noncrystalline gel can be prepared with 94 SiO₂ 6 TiO₂ (weight percent) glass composition.

Detailed investigations were not made on this system.